Efficient Spacing of Synchronous Communication Satellites

By HARRISON E. ROWE and ARNO A. PENZIAS

(Manuscript received April 10, 1968)

Satellites in equatorial circular synchronous orbit remain fixed with respect to an observer on the earth, while those in a circular synchronous orbit inclined with respect to the equator appear to move in a figure 8. A number of satellites can move on a given 8. Optimum packing for a single 8 is determined; the number of satellites per 8 increases as the 8 becomes larger and as the allowable closest approach between satellites decreases. Several packing schemes using multiple 8's, regularly spaced, are presented. For potential systems using frequencies above 12 GHz, with perhaps 1° closest approach between satellites, the best scheme described here permits approximately six times as many satellites as an equatorial system. An illustrative system serving North America has space for a total of 477 satellites, compared with 95 satellites if only equatorial orbits are allowed.

I. INTRODUCTION

When a satellite is in an orbit whose period is equal to that of the earth's rotation, it is said to be synchronous. A satellite in a synchronous, circular, equatorial (in the plane of the equator) orbit will appear stationary when viewed from the earth. The number of such satellites that can be used in a communication system in the same frequency band is limited by the directivity of the ground-based antennas.[1] The maximum number would be obtained by spacing them equally, at an angular separation just sufficient to keep crosstalk down to a tolerable level.

If the synchronous orbit is inclined to the equator, a satellite will no longer appear stationary when viewed from the earth, but will appear to move in a figure 8. By placing several satellites in a single 8, and spacing different 8's regularly along the equator, a greater number of synchronous communication satellites can be used than with an equatorial orbit alone.

A price must be paid for increasing the number of synchronous satellites by using inclined circular orbits:

(*i*) The earth-based antennas must track the satellites.

(*ii*) The satellite-based antennas must track the earth stations.

(*iii*) As the angle of inclination of the orbits is increased (in order to increase the number of satellites), the range of latitudes on earth within which the satellites will always be visible decreases.

In this paper we study optimum ways of packing satellites on inclined circular synchronous orbits, and determine the maximum number of such satellites that can be used under various conditions, assuming:

(*i*) Strictly circular, synchronous orbits, with consequent uniform satellite velocity.

(*ii*) Each satellite is usable at all times; that is, each satellite remains in view of ground stations located as far north as the Canadian-United States border, over a strip of substantial east-west width.

(*iii*) If the angular separation between any two satellites exceeds a certain minimum value, the crosstalk requirements will be satisfied. This minimum value is a parameter in the analysis.

(*iv*) The angular separation between satellites is computed as seen from the center of the earth.

These assumptions have the following corresponding consequences for this analysis:

(*i*) The problem is a kinematic or geometric one, rather than one in mechanics as if elliptical orbits, the oblateness of the earth, the effects of the moon, and so on, were considered. (Notice that we do not consider synchronous elliptical orbits.) This assumption implies that the satellites have sufficient on-board fuel to correct their orbits for various small perturbations (such as those mentioned above) over the expected life of the satellites, in addition to any fuel needed to track the earth stations if this is done by mechanically rotating the satellites (rather than by electronic beam-steering of the satellite antennas).

(*ii*) Assumption *ii* guarantees that there need be no switching from one satellite to another in such a communication system; this establishes a convenient bound on the present investigation. Once switching from one satellite to another is allowed, the system complexity appears to have no natural bound; one could theoretically fill the sky with satellites, and find a convenient one somewhere.

(*iii*) The minimum separation assumption avoids a detailed analysis of crosstalk. Such an analysis would have to include, for example, the type of modulation (AM, FM, PCM, and so on), the (angular) distances to all the satellites in the neighborhood of the one under study, the location of the ground stations, ground- and satellite- based antenna patterns, and the like.

(*iv*) By computing separation relative to the center of the earth, we neglect the small corrections which depend on the location of the ground stations; these corrections in satellite separation can vary between zero and as much as +18 percent in the worst case, as shown in Appendix C (see also Fig. 1 or 2, discussed below). However, assumption *iv* leads to simple, exact expressions for almost all of the interesting results.

Figures 1 and 2 show to scale the earth and a synchronous satellite, at declinations of 25° and 30° south latitude. The latitudes of repre-

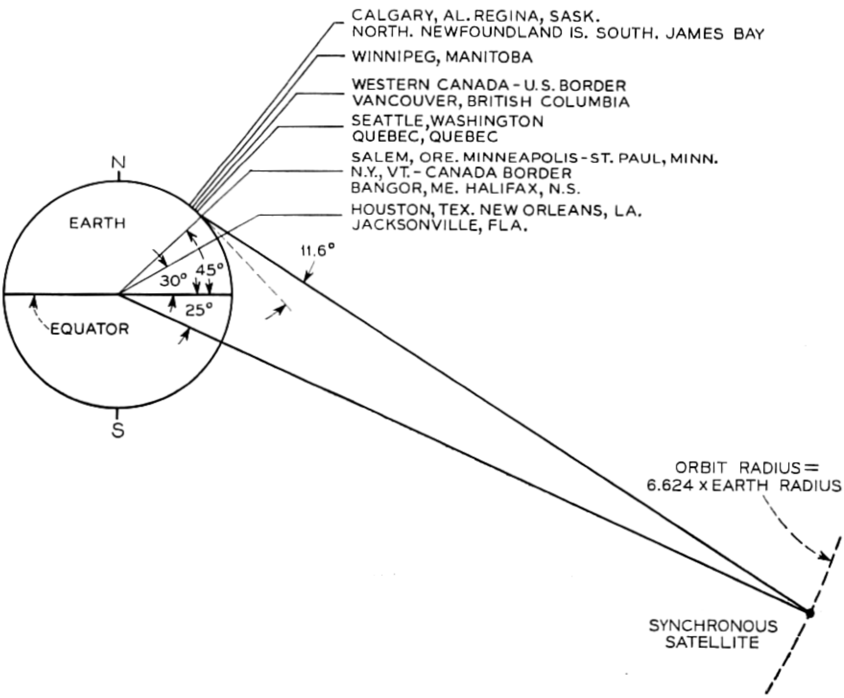

Fig. 1 — Synchronous satellite on an inclined orbit; southernmost declination = inclination = 25°.

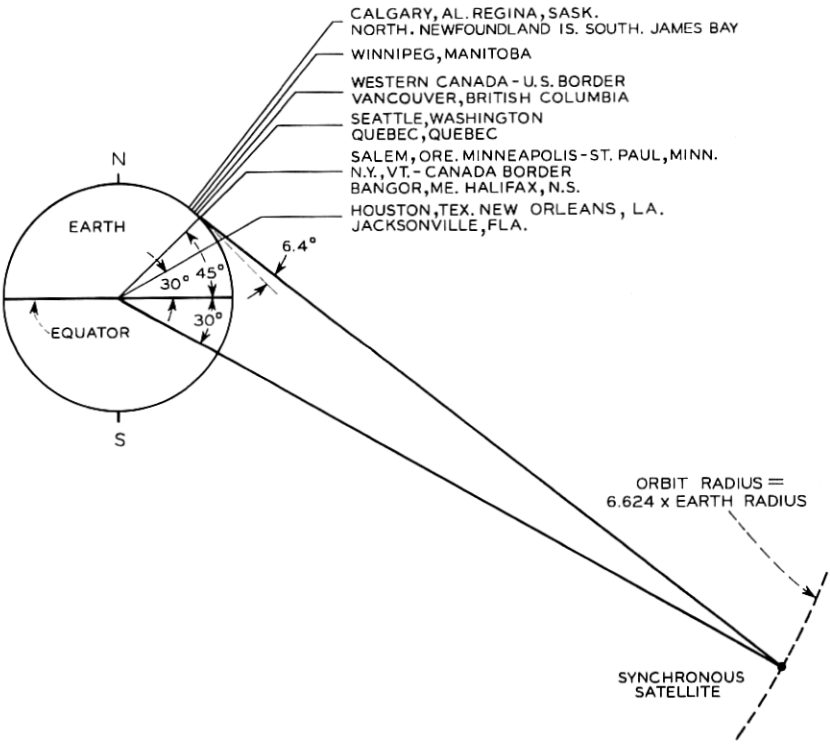

Fig. 2 — Synchronous satellite on an inclined orbit; southernmost declination = inclination = 30°.

sentative points in the United States and Canada are shown. Much of the United States is south of 45° north latitude; a ground station at this latitude will observe a synchronous satellite at the same longitude (as the ground station) at an elevation of 11.6° (Fig. 1) or 6.4° (Fig. 2) above the horizon. The smaller the satellite elevation the greater the path length lying within the atmosphere, with attendant greater rain attenuation, wavefront distortion, and other atmospheric effects.

Section II indicates that the extreme value of latitude (north and south) attained by a synchronous satellite is equal to its orbit's angle of inclination from the equator. Figures 1 and 2 suggest that the maximum angle of inclination of interest for the United States is about 30°. Such large angles will probably rule out major parts of Canada. However, in the systems described below, 8's containing several satellites each will be regularly spaced along the equator, separated by a smaller number of satellites in equatorial orbit equally spaced between the 8's. These equatorial satellites could probably be used to serve the lighter traffic to the more northern regions of North America or the more southern regions of South America, while both the figure 8 satellites and the equatorial satellites serve the heavy traffic within the continental United States.

II. GEOMETRY OF INCLINED, SYNCHRONOUS ORBITS

Let us compute the angular separation between satellites as seen from the center of the earth (assumption *iv*, Section I). This permits the calculation of all desired quantities by the straightforward use of the results of spherical trigonometry. By convention in spherical trigonometry, great circle distances on a sphere are measured by the angle they subtend at the center of the sphere; we use this convention throughout this article without further comment. By convention, with one principal exception, all lines drawn on the surface of a sphere in any figure of this article are great circles; the exception is the 8 described in the Introduction. Thus, longitude lines are allowed, while latitude lines are not.

Figure 3 shows the earth with north and south poles, the equator, and the projection on the earth of a (circular) synchronous orbit, inclined at an angle α to the equatorial plane, passing through the

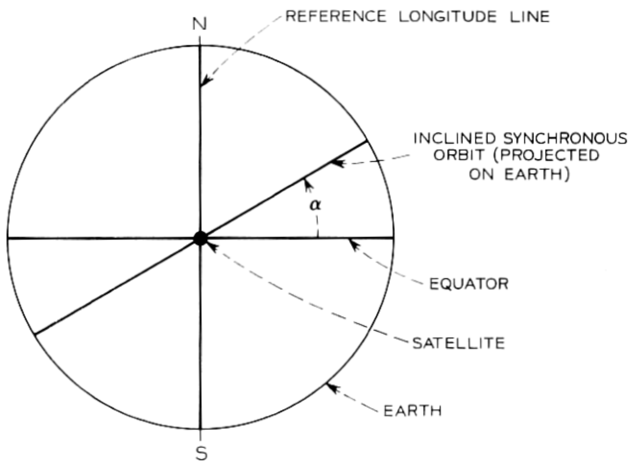

Fig. 3 — Reference point for satellite. $c = 0°$.

equator at its midpoint as seen by the observer. Since the orbit is viewed edge-on, it appears as a straight line rather than as an ellipse. A satellite is shown on the orbit line as a heavy dot. At the instant shown in Fig. 3, the satellite is at the intersection of the orbit with the equator; this configuration provides a convenient reference from which to measure time (or, equivalently, rotation). Finally, a longitude line is shown as a convenient reference on the earth, passing through the point on the equator which the satellite crosses; this also appears as a straight line in Fig. 3, since the plane of this longitude line contains the observer at this particular instant.

Figure 4 shows the satellite and the earth after some time has evolved: after the earth and the satellite have travelled an (angular) distance c. Of course, c will vary linearly with time in all of the following, increasing by 2π radians or 360° in one day. In Fig. 4, $c = \pi/4$ radians $= 45°$. Since both the satellite and the point on the equator that coincided with it when the satellite crossed the equator have travelled a distance $c < 90°$, the satellite will lie to the left to the reference longitude line, on the dashed longitude line shown in Fig. 4. When $c = 90°$ the satellite will have caught up with the longitude line and have attained its maximum north latitude (at the right-hand edge of the earth in Fig. 4). As c increases further the satellite will get ahead of the longitude line and start south; at $c = 180°$ the satellite crosses the equator and the longitude line simultaneously, the situation being as shown on Figure 3 except that satellite and longitude line lie on the far side of the earth. For $180° < c < 360°$ the above sequence is simply repeated symmetrically below the equator.

It is clear from the above description that such a satellite will move in a figure 8 as seen from the earth. Figures 5a and b illustrate this 8 pattern superimposed on Figs. 3 and 4.

The geometric parameters that describe the 8 are defined in Fig. 4, where we recall that all (great circle) distances, namely, c, l, a, e, and ψ, are measured by the angle they subtend at the center of the sphere. l is the latitude of the satellite, e the longitude of the satellite measured with respect to a fixed observer located at the point on the orbit where it crosses the equator, ψ is the relative longitude of the satellite measured with respect to an observer on the earth at the equator and the reference longitude line, a is the great circle distance from this earth observer to the satellite, and ϵ the relative angle (azimuth) between the earth observer's north and the satellite; a and ϵ correspond to local polar coordinates fixed to the surface of the earth.

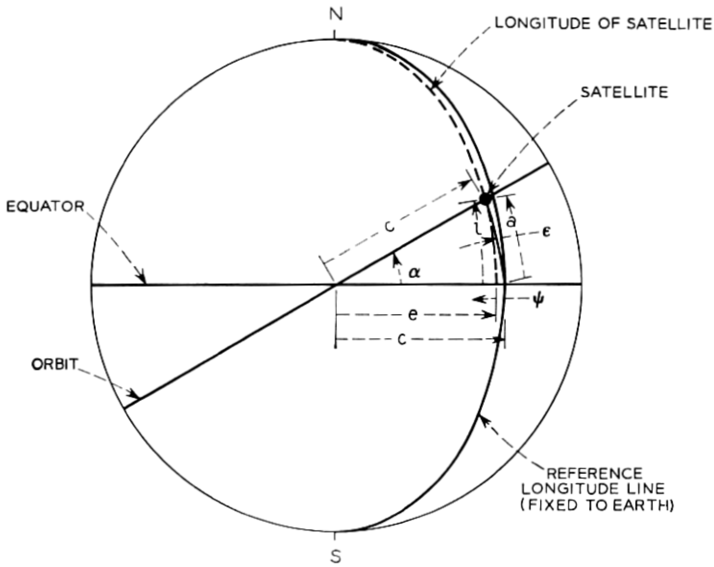

Fig. 4 — Satellite at some later time than Fig. 3. $c = 45°$.

In Fig. 4 and subsequent figures we adopt the convention that dimensions marked with two arrows are regarded as positive quantities; those with only a single arrow are positive in the direction of the arrow, and negative in the opposite direction.

Figure 6 shows an enlarged drawing of the 8 of Fig. 5b viewed from directly overhead, indicating those parameters of Fig. 4 that are measured relative to the earth observer. In addition, x measures the great circle distance from the satellite to the reference longitude, and

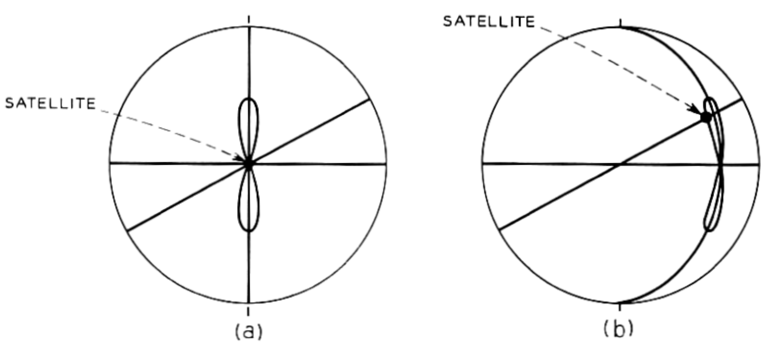

Fig. 5 — Figure 8 pattern. (a) $c = 0°$ as in Fig. 3; (b) $c = 45°$ as in Fig. 4.

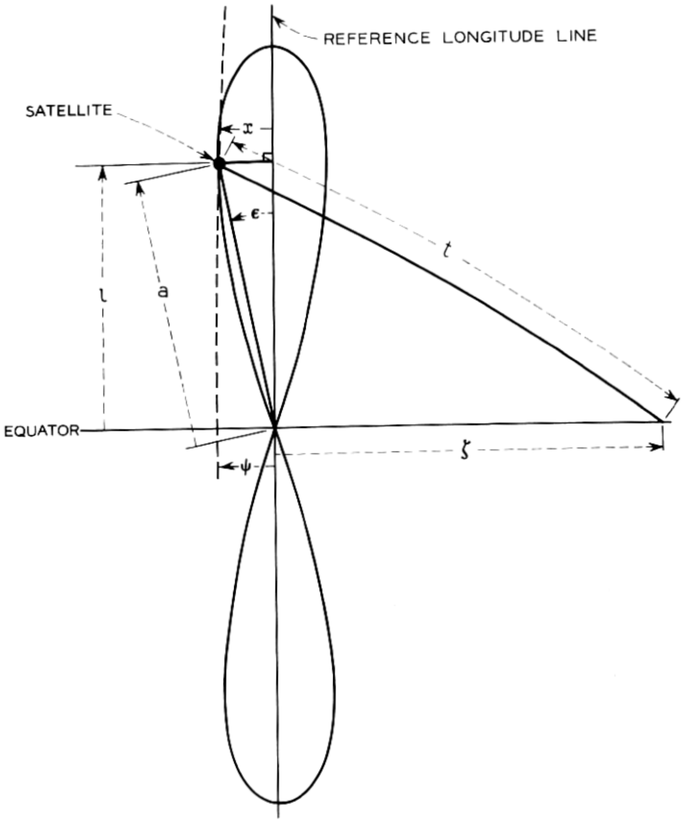

Fig. 6 — Enlarged 8 with relative geometric parameters. $c = 45°$.

t the (great circle) distance from the satellite to a point on the equator a distance ζ from the "cross" of the 8.*

The following results hold true for the parameters of Fig. 4 and 6:

$$\sin \frac{a}{2} = \sin \frac{\alpha}{2} \cdot \sin c. \tag{1}$$

$$\sin \epsilon = \frac{\sin \frac{\alpha}{2} \cdot \cos c}{\left(1 - \sin^2 \frac{\alpha}{2} \cdot \sin^2 c\right)^{\frac{1}{2}}}. \tag{2}$$

* The instant illustrated in Fig. 6 ($c = 45°$) is rather special, in that x has its maximum value and the dashed longitude line passing through the satellite is almost tangent to the 8. These conditions obviously do not hold in general.

$$\sin l = \sin \alpha \cdot \sin c. \tag{3}$$

$$\sin \psi = \frac{\sin^2 \frac{\alpha}{2} \cdot \sin 2c}{(1 - \sin^2 \alpha \cdot \sin^2 c)^{\frac{1}{2}}}. \tag{4}$$

$$\sin e = \frac{\cos \alpha \cdot \sin c}{(1 - \sin^2 \alpha \cdot \sin^2 c)^{\frac{1}{2}}}. \tag{5}$$

$$e + \psi = c. \tag{6}$$

$$\sin x = \sin^2 \frac{\alpha}{2} \cdot \sin 2c. \tag{7}$$

$$\cos t = \cos^2 \frac{\alpha}{2} \cdot \cos \zeta + \sin^2 \frac{\alpha}{2} \cdot \cos (2c + \zeta). \tag{8}$$

Next, we consider the (great circle) separation of two satellites travelling on the same 8. While these satellites lie on the same 8, they lie on different orbits. The geometry of this situation is illustrated in Fig. 7. One orbit is viewed edge-on, as in Figs. 4 and 5; the other orbit's plane is inclined, and so it appears as an ellipse in this figure. The

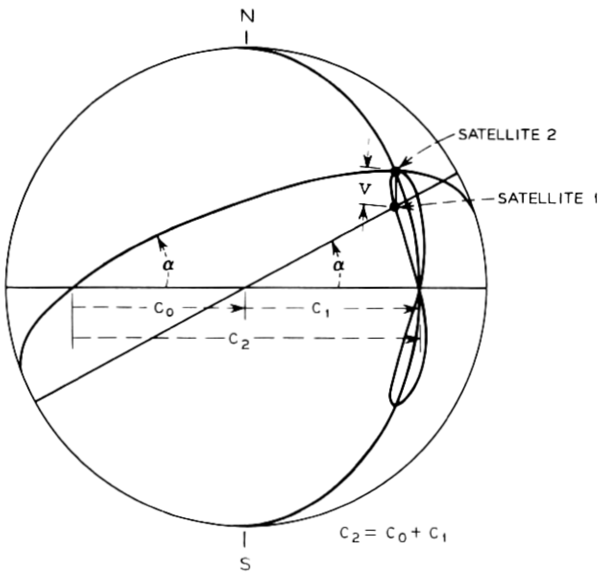

Fig. 7 — Two satellites on the same 8. $c_1 = 45°$ $c_2 = 90°$.

distance between the two satellites is denoted by v. The two satellites have phases c_1 and c_2, with phase difference c_0; c_1 and c_2 of course have the same linear variation with time, while c_0 is fixed. Then the distance between the two satellites is given by

$$\sin^2 \frac{v}{2} = \sin^4 \frac{\alpha}{2} \cdot \sin^2 c_0 + \sin^2 \alpha \cdot \sin^2 \frac{c_0}{2} \cdot \cos^2 \left(c_1 + \frac{c_0}{2}\right),$$

$$c_0 = c_2 - c_1 . \qquad (9)$$

Equation 9 yields equation 1 by setting $v = a$, $c_1 = c$, $c_2 = 0$.

Consider next Fig. 8, which shows two identical 8's spaced by a distance ζ along the equator. The parameter u denotes the (great circle) distance between symmetrically located points at the same latitude. u is illustrated at two representative times, indicated as u_1 and u_2. The corresponding ranges for c_2 are shown on Figure 8, where c_2 is the phase parameter on the right 8. Then

$$\sin \frac{u}{2} = \cos^2 \frac{\alpha}{2} \cdot \sin \frac{\zeta}{2} - \sin^2 \frac{\alpha}{2} \cdot \sin \left(2c_2 - \frac{\zeta}{2}\right). \qquad (10)$$

Our final result contains some of the preceding results as special cases. Consider two 8's of differing size, characterized by parameters α_1 and α_2, spaced by a distance ζ along the equator. This situation is illustrated in Fig. 9. While for clarity the two 8's in Fig. 9 have been drawn as not overlapping, this is not a necessary restriction in the

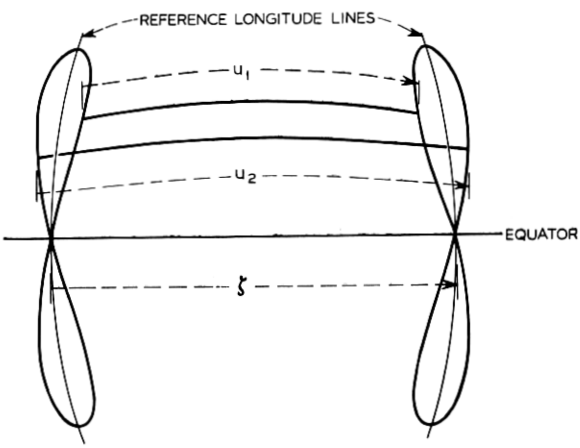

Fig. 8 — Distance between identical 8's at the same latitude. c_2 = phase parameter on right-hand 8. u_1: $0 < c_2 < 90°$; u_2: $90° < c_2 < 180°$.

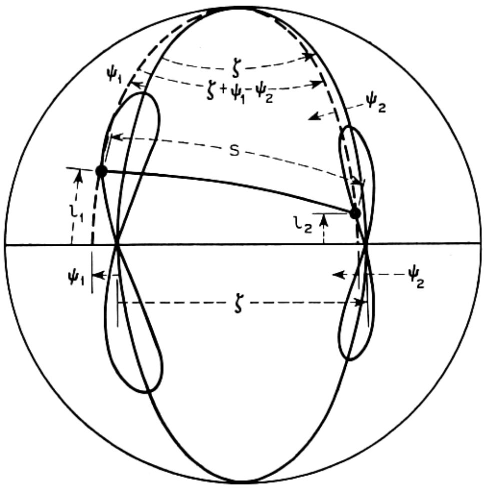

Fig. 9 — Distance between two satellites with arbitrary phases, located on different 8's of arbitrary sizes.

following. Consider a satellite on each 8, having phases c_1 and c_2. Then the great-circle separation s between these two satellites is given by

$$\begin{aligned}\cos s = {} & \cos \zeta \cdot \cos^2 \frac{\alpha_1}{2} \cdot \cos^2 \frac{\alpha_2}{2} \\ & + \frac{\sin \alpha_1 \cdot \sin \alpha_2}{2} [\cos (c_2 - c_1) - \cos (c_2 + c_1)] \\ & + \sin^2 \frac{\alpha_1}{2} \cdot \cos^2 \frac{\alpha_2}{2} \cdot \cos (2c_1 + \zeta) \\ & + \sin^2 \frac{\alpha_2}{2} \cdot \cos^2 \frac{\alpha_1}{2} \cdot \cos (2c_2 - \zeta) \\ & + \sin^2 \frac{\alpha_1}{2} \cdot \sin^2 \frac{\alpha_2}{2} \cdot \cos (2c_2 - 2c_1 - \zeta). \end{aligned} \tag{11}$$

The following specializations of equation 11 yield the indicated above results:

Equation	*Parameters in Equation 11*
1	$s = a : \alpha_1 = \alpha_2 = \alpha,\ c_1 = 0,\ c_2 = c,\ \zeta = 0.$
8	$s = t : \alpha_1 = \alpha,\ c_1 = c,\ c_2 = 0$ or $\alpha_2 = 0.$
9	$s = v : \alpha_1 = \alpha_2 = \alpha,\ \zeta = 0.$
10	$s = u : \alpha_1 = \alpha_2 = \alpha,\ c_1 = \pi - c_2.$

One final specialization of this result is of interest, in which the two 8's have the same size. For convenience we denote the phase difference for the two satellites (each on its separate 8) by c_0, as in equation 9. Thus setting

$$\begin{aligned} \alpha_1 &= \alpha_2 = \alpha, \\ c_2 &= c_1 + c_0 , \end{aligned} \tag{12}$$

in equation 11, yields

$$\begin{aligned} \sin^2 \frac{s}{2} = {} & \left[\cos^2 \frac{\alpha}{2} \cdot \sin \frac{\zeta}{2} + \sin^2 \frac{\alpha}{2} \cdot \sin \left(c_0 - \frac{\zeta}{2}\right)\right]^2 \\ & + \left[\sin \alpha \cdot \sin \left(\frac{c_0 - \zeta}{2}\right) \cdot \cos \left(c_1 + \frac{c_0}{2}\right)\right]^2 . \end{aligned} \tag{13}$$

This relation also reduces to equation 9 for $\zeta = 0$, in an obvious way.

All of the above results are exact; no small-angle or any other approximations have been made. Their derivation is sketched in Appendix A. They are necessary for calculating minimum satellite separation in various packing schemes, discussed in Sections III through V.

III. OPTIMUM PACKING ON A SINGLE 8

Equation 9 shows that the separation between two satellites on the same 8 varies periodically with time in a simple way. This relation, together with Fig. 7, readily permits the exact calculation of the closest approach or minimum separation $v_{\min}$ and the corresponding satellite phases $c_{1\,\min}$ and $c_{2\,\min}$ at which it occurs.

$$\begin{aligned} c_{1\,\min} &= \pm\frac{\pi}{2} - \frac{c_0}{2}, \qquad c_{2\,\min} = \pm\frac{\pi}{2} + \frac{c_0}{2}, \\ \sin \frac{v_{\min}}{2} &= \sin^2 \frac{\alpha}{2} \cdot |\sin c_0|, \qquad c_0 = c_2 - c_1 , \end{aligned} \tag{14}$$

where all c's are measured in radians.

Figure 10 illustrates the satellite positions at minimum separation for two representative cases. Minimum separation for any two satellites occurs when the two lie at the same latitude. (A similar study for maximum separation is easily performed; maximum separation is illustrated in Fig. 11 for the same satellite distributions shown in Fig. 10.)

Consider N satellites placed on an 8, with phases $c_1, c_2, \cdots c_N$, all

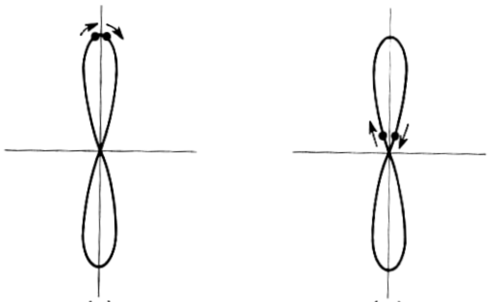

Fig. 10 — Satellite positions at minimum separation. Identical (minimum) separation in both figures. (a) $c_0 = 20°$, (b) $c_0 = 160°$.

having the same linear variation with time t (but different values at $t = 0$); each c increases by 2π radians in one day. We represent the phases of these satellites by points on a circle at angles $c_1, c_2, \cdots c_N$. This pattern of points will rotate uniformly counterclockwise at one revolution per day, and the relative angular positions of these representative points will remain constant with time. One such point is shown in Fig. 12 at angle c_1. Suppose the desired minimum separation between any two satellites on this 8 is specified as $v_{\min}$. The separation between the satellite with phase c_1 in Fig. 12 and any other satellite will equal or exceed $v_{\min}$ if (equation 14)

$$| \sin c_0 | \geqq \frac{\sin \frac{v_{\min}}{2}}{\sin^2 \frac{\alpha}{2}} \equiv \sin c_{0\,\min}, \tag{15}$$

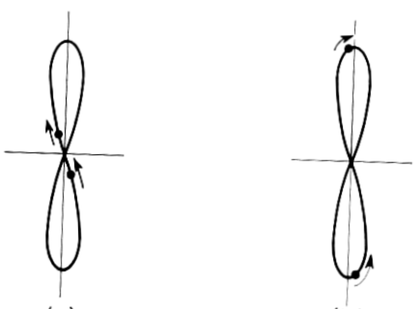

Fig. 11 — Satellite positions at maximum separation. (a) $c_0 = 20°$, (b) $c_0 = 160°$.

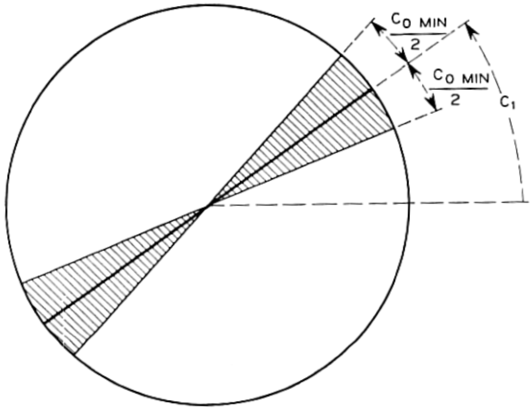

Fig. 12 — Phase of a satellite with associated sector. $c_{0\,\min}$ given by equation 15.

where c_0 is now regarded as the phase separation between the satellite under study (No. 1) and any other satellite on this 8.

Suppose we associate with the point c_1 on Fig. 12 a shaded sector of angle $c_{0\,\min}$ centered on c_1, and the image of this sector reflected through the axis. Next imagine a second representative point placed on the circle at angle c_2, with a similar pair of shaded sectors. If the shaded regions corresponding to the two representative points do not overlap, equation 15 will be satisfied and $v \geqq v_{\min}$. Additional points c_3, c_4, $\cdots$ may be similarly added such that none of the shaded areas overlap, and the separation v between any pair of satellites at any time will be guaranteed to exceed $v_{\min}$.

It is clear that efficient packing requires adjacent shaded areas to just touch; optimum packing will be attained if the entire area of the circle is filled with shaded sections, that is, if

$$N = \frac{\pi}{c_{0\,\min}}, \tag{16}$$

where N is the total number of satellites ($c_{0\,\min}$ is in radians). The minimum separation with optimum packing for N satellites on the 8 is therefore given by

$$\sin \frac{v_{\min}}{2} = \sin^2 \frac{\alpha}{2} \cdot \sin \frac{\pi}{N}. \tag{17}$$

Equation 17 is illustrated in Fig. 13, where the pertinent angles, $v_{\min}$ and α, have been expressed in degrees rather than in radians.

It remains only to illustrate the possible geometric distributions of satellites corresponding to the optimum packing of equation 17. Figure 14 illustrates the geometry for an odd number of satellites, $N = 3$. The time has been arbitrarily selected so that one satellite is located at the "cross" of the 8, at zero phase. In Fig. 14a the satellites have been uniformly distributed over half the circle; this may be regarded as the canonical optimum distribution, with others derived from it. The discussion in connection with Fig. 12 makes it clear that an equivalent optimum distribution results from shifting the phase of any of the satellites by 180°.

Figure 14b shows a possible alternative. In general, if the even numbered satellites for N odd are shifted by 180°, then the satellites will be equally-spaced in phase over the entire circle, as illustrated in Fig. 14b. This may be regarded as a second canonical distribution, of subsequent interest for an odd total number of satellites on the 8. Other distributions are clearly possible, although not for $N = 3$. Figure

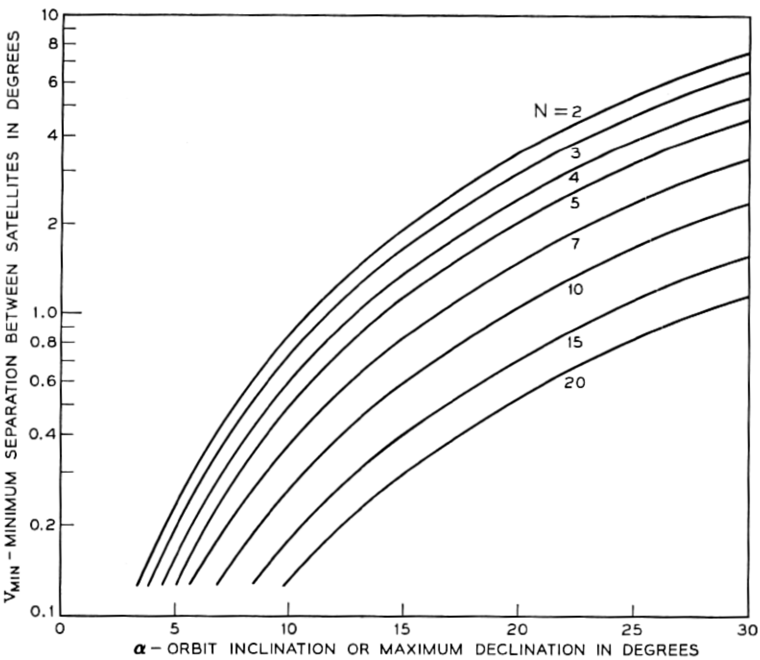

Fig. 13 — Closest approach of satellites on a single 8 with optimum packing. See equation 17. N = number of satellites on a single 8.

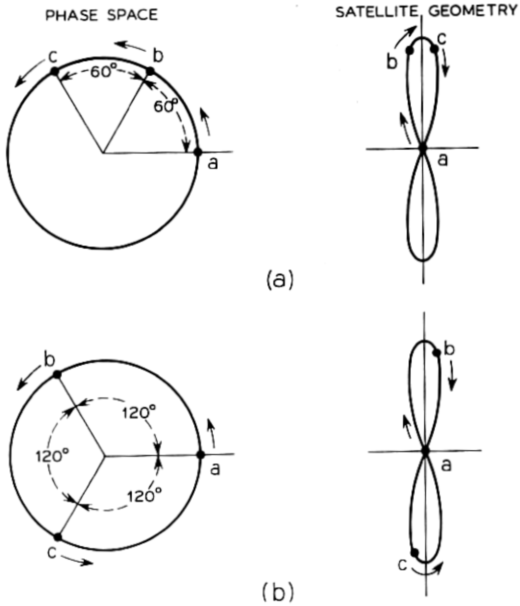

Fig. 14 — Optimum packing for $N = 3$. Uniform phase spacing over (a) 180° and (b) 360°.

15 shows the satellites at different times for the two situations in Fig. 14; the instants of closest approach indicated in Fig. 15 have identical minimum separation.

In general, the optimum uniform distribution over 180° is given by

$$c_p = c_1 + (p - 1)\frac{\pi}{N}, \qquad p = 1, 2, \cdots N;$$

uniform phase spacing over 180° (18)

For an odd number of satellites, we have alternatively

$$c_p = c_1 + 2(p - 1)\frac{\pi}{N}, \qquad p = 1, 2, \cdots N, \qquad N \text{ odd};$$

uniform phase spacing over 360°. (19)

(The c_p are measured in radians in equations 18 and 19.)

All equivalent optimum packing schemes, for a given N and α, result in the identical $v_{\min}$, that is, minimum separation or closest approach between any pair of satellites at any time. However, other geometric properties (such as the average spacing) may vary widely for the various packing schemes. The minimum separation is the only parameter considered here by assumption *iii* of Section I. The systems implications of different packing schemes are discussed briefly in Section VII.

The results in this section, giving optimum packing of satellites on a single 8, are exact (subject to the assumptions of Section I). They are used in Sections IV and V to determine the best way to stack 8's under various conditions and so determine the maximum number of synchronous satellites that can be used in an extended portion of the sky, subject to different constraints.

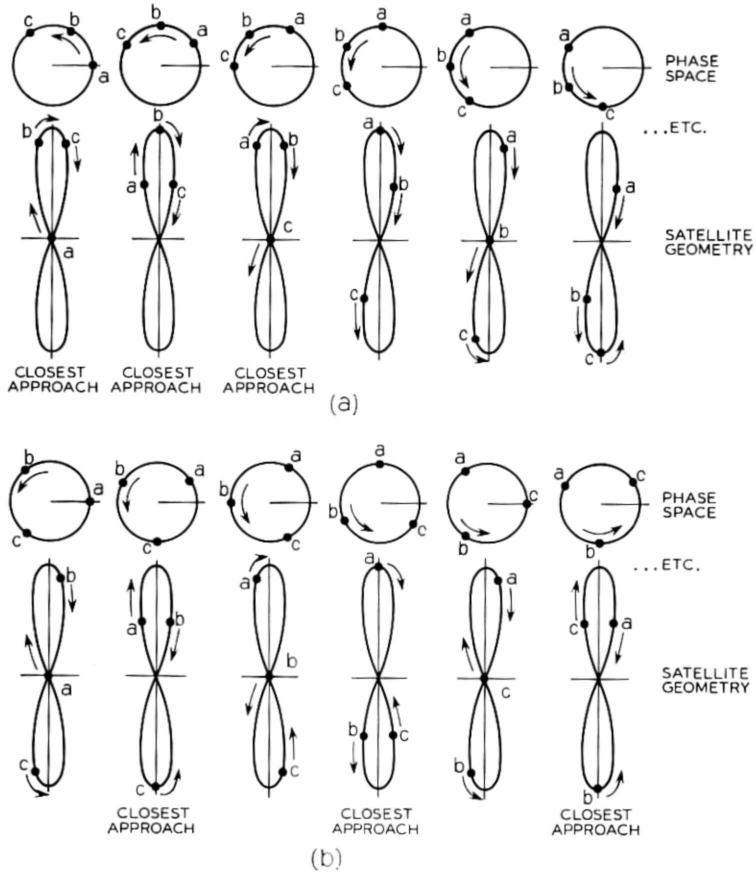

Fig. 15 — Satellite motion for $N = 3$, optimum packing. Phase increment = 30°. Uniform phase spacing over (a) 180° and (b) 360°.

IV. OPTIMUM PACKING—UNSYNCHRONIZED, SEPARATED 8'S

Assume that we are given:

(*i*) The minimum allowable separation (that is, the closest approach) between any two satellites $= v_{\min}$.

(*ii*) The maximum allowable orbit inclination (equal to the maximum declination of the satellites) $= \alpha_{\max}$.

Optimum packing on a single 8 has been studied in Section III. We seek to increase the number of synchronous satellites (over the number available in an equatorial system, that is, using a synchronous equatorial orbit only) by using such 8's spaced equally along the equator.

The canonical distribution for N satellites on an 8 is given by equation 18 for general N, or for odd N by equation 19 (with other distributions possible as mentioned in Section III). For a given N and a given $v_{\min}$, it is obviously desirable to use the minimum α allowed, given by equation 17 or Fig. 13, to minimize the space occupied by these N satellites. This equation and figure yield the maximum number of satellites $N_{\max}$ that can be placed on a single 8 for a specified $v_{\min}$, $\alpha_{\max}$. We therefore consider the improvement possible for $N = 2, 3, \cdots N_{\max}$, with corresponding $\alpha = \alpha_1, \alpha_2, \cdots \alpha_{N_{\max}} \leqq \alpha_{\max}$ given by equation 17 or Fig. 13.

It might have been anticipated for specified $v_{\min}$, $\alpha_{\max}$ that the largest number of satellites per 8 (that is, $N_{\max}$) will yield the greatest improvement. This is indeed true for the smaller values of $N_{\max}$ (perhaps $N_{\max} < \sim 10$). Although cases exist for $N_{\max} > 13$ where $N_{\max} - 1$ or $N_{\max} - 2$ are slightly better, the difference is not significant. Consequently, it seems likely that the configuration corresponding to $N_{\max}$, $\alpha_{N\max}$ will either be optimum or very close to it.

Assume that 8's each with N optimally packed satellites are spaced equally along the equator. The N satellites on each 8 must of course be carefully synchronized; however, we assume in this section that no synchronization will be required between the relative phase of groups of satellites on different 8's. Two such 8's are shown in Fig. 16. The minimum (great circle) distance between these two 8's, $u_{\min}$, must equal or exceed $v_{\min}$ in order that the closest approach between satellites on different 8's equals or exceeds $v_{\min}$. The distance between 8's along the equator is denoted by ζ; its minimum value, $\zeta_{\min}$, corresponds to $u_{\min} = v_{\min}$, that is, the minimum distance between 8's equal to $v_{\min}$. Two points are shown on the equator, whose minimum distance to their respective 8's, $t_{\min}$, is set equal to $v_{\min}$; these points are a distance ζ' from each 8 measured along the equator. There is a

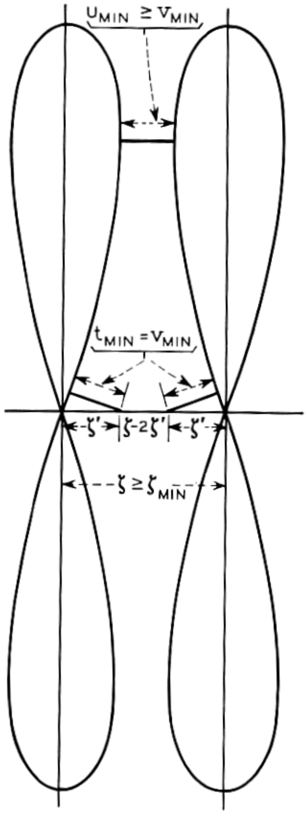

Fig. 16 — Geometry of adjacent 8's. $\xi = \xi_{min}$ for $u_{min} = v_{min}$. v_{min} = closest approach among N optimally packed satellites on each 8.

portion of equator $\zeta - 2\zeta'$ long, available for additional synchronous equatorial satellites, separated from each other by a distance v_{min}.*

We now define an improvement factor I that measures the effective-

* The possibility of using smaller 8's, rather than only equatorial satellites between the major 8's, has also been considered. However, a crude analysis that replaces sines of small angles by their arguments and effectively neglects the curvature of the sphere shows that for $N < 16$ there is not enough room for a small 8 containing even two satellites between the two main 8's spaced at the minimum distance ζ_{min}. This suggests that small 8's will be of no value for the range of interest in this paper ($N < \sim 25$—see Fig. 13), although the packing can obviously be improved for very large N ($N \gg 25$) by this means. A precise investigation of this problem requires a detailed study based on equation 11.

ness of our satellite packing schemes as follows:

$$I = \frac{\text{number of satellites per unit of longitude for packing scheme under consideration}}{\text{number of satellites per unit of longitude using equatorial orbit only (that is, without 8's)}}, \tag{20}$$

with closest approach the same in numerator and denominator. If E denotes the number of equatorial satellites between adjacent 8's, then from Fig. 16

$$E = \left\{ \frac{\zeta - 2\zeta'}{v_{\min}} \right\} + 1 \tag{21}$$

where the { } denote "the largest integer contained in" the enclosed expression.* For the packing scheme under consideration $N + E$ satellites occupy a longitude interval ζ. For an equatorial system one satellite occupies a longitude interval $v_{\min}$, so that effectively $\zeta/v_{\min}$ satellites occupy a longitude interval ζ. Therefore from equation 20 and 21 the improvement factor is

$$I = \frac{N + 1 + \left\{ \dfrac{\zeta - 2\zeta'}{v_{\min}} \right\}}{\dfrac{\zeta}{v_{\min}}}, \qquad \zeta \geqq \zeta_{\min} . \tag{22}$$

(Notice that the denominator of equation 22 need not be an integer, as must the numerator.)

I of equation 22 is a function of ζ. Suppose we first set $\zeta = \zeta_{\min}$, that is, place adjacent 8's as close as possible without causing (asynchronously phased) satellites on the two 8's to approach each other closer than $v_{\min}$. In general the E equatorial satellites of equation 21 will not exactly fill up the available space on the equator of length $\zeta_{\min} - 2\zeta'$; that is, the quantity $(\zeta_{\min} - 2\zeta')/v_{\min}$ will not be exactly an integer.

We now inquire if increasing the spacing ζ between adjacent 8's beyond its minimum value can improve I of equation 22. The answer is sometimes yes, sometimes no. Intuitively, if $(\zeta_{\min} - 2\zeta')/v_{\min}$ in the numerator of equation 22 is only slightly greater than an integer, that is, if there is only a little extra room on the equator at minimum distance between 8's, then $\zeta = \zeta_{\min}$ gives the largest improvement

* Equation 21 is obviously valid only when it predicts $E \geqq 0$; it will appear below that $E \geqq 1$.

factor I. However, if $(\zeta_{\min} - 2\zeta')/v_{\min}$ is only slightly less than an integer, in other words, if there is almost enough room on the equator for an extra satellite for $\zeta = \zeta_{\min}$, it pays to increase ζ a little beyond $\zeta_{\min}$ to just accommodate the extra equatorial satellite. It clearly never pays to increase ζ further.

Consequently, we evaluate I and E of equation 22 and 21 for the following two values of ζ:

$$\zeta_1 = \zeta_{\min}, \tag{23}$$

$$\zeta_2 = 2\zeta' + v_{\min} + v_{\min}\left\{\frac{\zeta_{\min} - 2\zeta'}{v_{\min}}\right\}. \tag{24}$$

The corresponding improvement factors I_1 and I_2, with corresponding numbers of equatorial satellites E_1 and E_2, are:

$$I_1 = \frac{N + 1 + \left\{\dfrac{\zeta_{\min} - 2\zeta'}{v_{\min}}\right\}}{\dfrac{\zeta_{\min}}{v_{\min}}}; \qquad E_1 = \left\{\frac{\zeta_{\min} - 2\zeta'}{v_{\min}}\right\} + 1. \tag{25}$$

$$I_2 = \frac{N + 2 + \left\{\dfrac{\zeta_{\min} - 2\zeta'}{v_{\min}}\right\}}{\left\{\dfrac{\zeta_{\min} - 2\zeta'}{v_{\min}}\right\} + \dfrac{2\zeta'}{v_{\min}} + 1}; \qquad E_2 = \left\{\frac{\zeta_{\min} - 2\zeta'}{v_{\min}}\right\} + 2. \tag{26}$$

The optimum improvement factor is the greater of I_1 and I_2. It remains only to evaluate equation 25 and 26 from the results of Sections II and III.

From equation 17

$$\sin\frac{v_{\min}}{2} = \sin^2\frac{\alpha}{2}\cdot\sin\frac{\pi}{N}. \tag{27}$$

From equation 10 and Fig. 8

$$\sin\frac{u_{\min}}{2} = \cos^2\frac{\alpha}{2}\cdot\sin\frac{\zeta}{2} - \sin^2\frac{\alpha}{2}; \tag{28}$$

consequently,

$$\sin\frac{\zeta}{2} = \frac{\sin\dfrac{u_{\min}}{2}}{\cos^2\dfrac{\alpha}{2}} + \tan^2\frac{\alpha}{2}. \tag{29}$$

We set $u_{\min} \to v_{\min}$ and $\zeta \to \zeta_{\min}$ in equation 29 to obtain

$$\sin \frac{\zeta_{\min}}{2} = \tan^2 \frac{\alpha}{2} \left(1 + \sin \frac{\pi}{N}\right). \tag{30}$$

From equation 8 and Fig. 6, with $\zeta \to \zeta'$ to conform to the notation in this section and Fig. 16,

$$\cos t_{\min} = \cos^2 \frac{\alpha}{2} \cdot \cos \zeta' + \sin^2 \frac{\alpha}{2}. \tag{31}$$

Using the double-angle formula for the two cosines, this becomes

$$\sin \frac{t_{\min}}{2} = \cos \frac{\alpha}{2} \cdot \sin \frac{\zeta'}{2}\ ; \tag{32}$$

finally setting $t_{\min} \to v_{\min}$ in equation 32,

$$\sin \frac{\zeta'}{2} = \frac{\sin^2 \frac{\alpha}{2} \cdot \sin \frac{\pi}{N}}{\cos \frac{\alpha}{2}}. \tag{33}$$

Equations 27, 30, and 33 substituted in equations 25 and 26 permit evaluation of I (the improvement factor) and E (the corresponding number of satellites on the equator between 8's), as a function of N (the number of satellites per 8) and α (the orbit inclination or maximum declination of the satellites on the 8's), for the two interesting values of spacing (along the equator) between 8's given in equation 23 and 24. These results are plotted on Figure 17; equation 25 is shown by solid lines, and equation 26 by dashed lines.

Figures 13 and 17 used in conjunction determine the improvement factor for the present packing scheme. (Some values of N have been omitted in these figures for clarity, but may of course be supplied by the equations from which these figures were obtained.) Given $v_{\min}$ and $\alpha_{\max}$:

(*i*) On Fig. 13, find the largest value of N corresponding to $v_{\min}$ and $\alpha \leqq \alpha_{\max}$. Denote this value of N by $N_{\max}$, the associated value of α by $\alpha_{N_{\max}}$; $\alpha_{N_{\max}} \leqq \alpha_{\max}$.

(*ii*) On Fig. 17, find the two possible improvement factors (solid and dashed) corresponding to $N_{\max}$, $\alpha_{N_{\max}}$ and choose the larger. Read the associated number of equatorial satellites from the appropriate curve.*

* As mentioned at the beginning of this section, it is possible that a smaller value of $N < N_{\max}$ may yield a slightly, although not significantly, larger improvement factor. Fig. 17 makes it clear that this is possible only for large N, and of course for intermediate N not plotted in this figure.

A variety of possible types of behavior is illustrated in Fig. 17. For some N the solid curve always exceeds the dotted curve (for example, $N = 2, 3, 7, 10$) and the 8's should be spaced as closely as possible; for other N the reverse is true (as when $N = 5$) and the distance between 8's should be increased just enough beyond its minimum value to permit one additional satellite on the equator between each pair of 8's. In both these cases the number of equatorial satellites remains constant for all values of α shown.

There are still other cases where both types of the above behavior hold for a given N; for small values of α the 8's should be close-

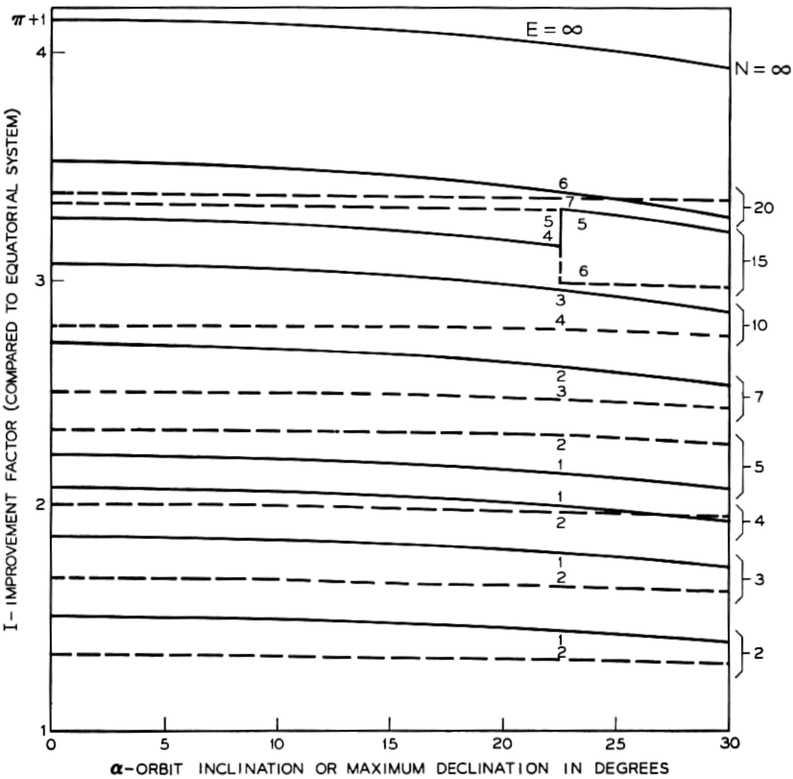

Fig. 17—Improvement factor for optimum satellite packing on unsynchronized, separated 8's. Use this figure in conjunction with Fig. 13. E = number of satellites on equator between two adjacent 8's. N = number of satellites on a single 8. ——— indicates minimum spacing between adjacent 8's; closest approach for adjacent 8's = closest approach for a single 8. (See fig. 13 and equation 25). – – – – indicates increased spacing between adjacent 8's that just permits 1 additional equatorial satellite. See equation 26.

spaced, for large α there should be an extra equatorial satellite (such as, $N = 4$, 20). Here the number of equatorial satellites increases by 1 at a critical value of α.

Finally, for $N = 15$ the behavior changes at a critical value of α in a different way. Here the number of equatorial satellites remains constant for all α shown. For small α the spacing between 8's should be increased to allow for an extra equatorial satellite, while for large α the 8's are close-spaced.

The above relations simplify as $\alpha \to 0$ or as $N \to \infty$. We have:

$\underline{\alpha = 0}$

$$I_1 = \frac{N + \left\{\dfrac{1}{\sin \dfrac{\pi}{N}}\right\}}{1 + \dfrac{1}{\sin \dfrac{\pi}{N}}}; \qquad E_1 = \left\{\frac{1}{\sin \dfrac{\pi}{N}}\right\}, \tag{34}$$

$$I_2 = \frac{N + 1 + \left\{\dfrac{1}{\sin \dfrac{\pi}{N}}\right\}}{2 + \left\{\dfrac{1}{\sin \dfrac{\pi}{N}}\right\}}; \qquad E_2 = \left\{\frac{1}{\sin \dfrac{\pi}{N}}\right\} + 1. \tag{35}$$

$\underline{N = \infty}$

$$I = I_1 = I_2 = \frac{\pi \sin^2 \dfrac{\alpha}{2}}{\sin^{-1} \tan^2 \dfrac{\alpha}{2}} + 1; \qquad \frac{E}{N} = \frac{\sin^{-1} \tan^2 \dfrac{\alpha}{2}}{\pi \sin^2 \dfrac{\alpha}{2}}. \tag{36}$$

It is clear from equation 36 that an upper bound on the improvement factor for the present packing scheme is $I = \pi + 1$, with $E/N = 1/\pi$. Figure 13 shows that this may be approached only for extremely small closest approach $v_{\min}$; hence practical improvement factors will be smaller.

V. OPTIMUM PACKING—SYNCHRONIZED, OVERLAPPING 8'S

In the packing schemes of Section IV, optimally-packed 8's are spaced far enough apart so that closest approach for satellites on adjacent 8's equals or exceeds closest approach for satellites on the same 8, for arbitrary relative phasing on different 8's. We now inquire if the number of satellites can be increased (for a given closest approach and orbit inclination or maximum declination) by careful relative phasing on 8's in such a way that they can lie closer together, and even overlap (with proper interleaving of satellites on different 8's). We restrict the present treatment to 8's of identical size (that is, identical orbit inclination α) for simplicity, with equatorial satellites between 8's as permitted.

The basic relation needed for this study is equation 13 (and equation 12), which shows that the separation between two satellites on different 8's (of the same size) varies periodically with time in a simple way. We denote this minimum separation by $s_{\min}$, occurring at satellite phases $c_{1\,\min}$ and $c_{2\,\min}$ on the left and right 8's (spaced by ζ along the equator), respectively. Then

$$c_{1\,\min} = \pm\frac{\pi}{2} - \frac{c_0}{2}, \qquad c_{2\,\min} = \pm\frac{\pi}{2} + \frac{c_0}{2},$$

$$\sin\frac{s_{\min}}{2} = \sin^2\frac{\alpha}{2}\cdot\left|\sin\left(c_0 - \frac{\zeta}{2}\right) + \cot^2\frac{\alpha}{2}\cdot\sin\frac{\zeta}{2}\right|, \tag{37}$$

$$c_0 = c_2 - c_1 .$$

We see that closest approach for satellites on two different 8's of the same size occurs when the two satellites attain the same latitude; this behavior was observed in Section III for two satellites on the same 8 (compare the top lines of equations 14 and 37). $s_{\min}$ of equation 37 reduces to $v_{\min}$ of equation 14 for $\zeta = 0$, the degenerate case in which the two 8's become identical.

Assume now that $s_{\min}$ is given. Equation 37 then determines two forbidden regions for c_0; for every satellite on the left (No. 1) 8, with phase c_1, two forbidden regions in phase space on the right (No. 2) 8 are established, that is, two ranges of c_2 within which no satellites may be placed. Thus, in addition to the self-phase-space of Section III (determined by equation 14), which governs packing on each 8 considered independently, a mutual-phase-space (determined by equation 37) must be considered for each pair of 8's lying closer than $\zeta_{\min}$ of Section IV (equation 30).

Figure 18 and 19 give a convenient geometric picture of this pair of forbidden regions. We assume each 8 of the pair considered to contain N optimally packed satellites, according to Section III. Then

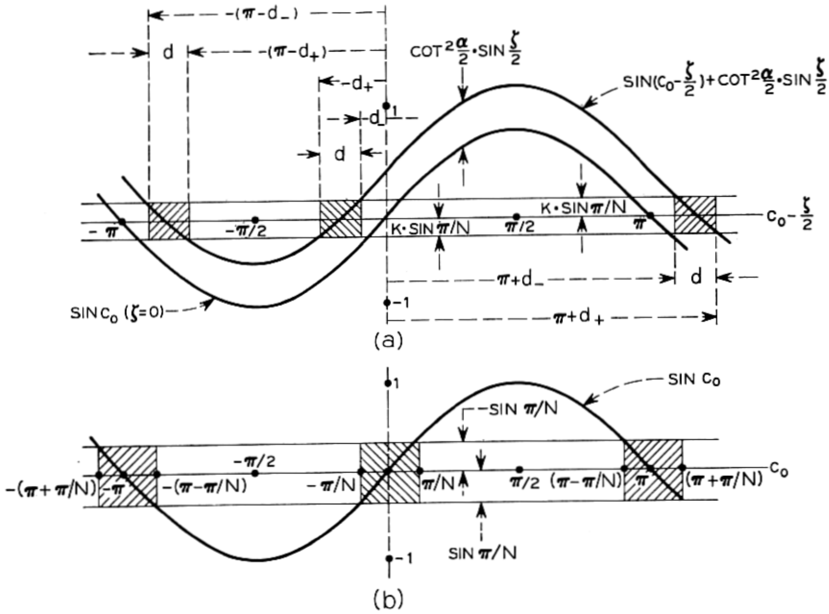

Fig. 18 — Forbidden region for relative phase between satellites on different 8's (equation 37). $N = 9$. (a) General case. $\cot^2 \alpha/2 \cdot \sin \zeta/2 = 0.5$ (separation about half that for two 8's just touching), $K = 0.6$. Enlarged portion of upper curve, containing forbidden region to left of origin, shown in Fig. 19. (b) Limiting case (single 8). $\zeta = 0$, $K = 1$. This curve is the same as the lower curve of (a).

closest approach on each 8 is $v_{\min}$, given by equation 17 as

$$\sin \frac{v_{\min}}{2} = \sin^2 \frac{\alpha}{2} \cdot \sin \frac{\pi}{N}. \tag{38}$$

We assume that $s_{\min}$, closest approach between 8's, is less than $v_{\min}$, according to the following relation for later convenience.

$$\sin \frac{s_{\min}}{2} = K \cdot \sin \frac{v_{\min}}{2}, \qquad 0 < K < 1. \tag{39}$$

Thus,

$$\sin \frac{s_{\min}}{2} = \sin^2 \frac{\alpha}{2} \cdot K \sin \frac{\pi}{N}, \qquad 0 < K < 1. \tag{40}$$

For zero spacing, $\zeta = 0$ (Fig. 18b), the principal forbidden regions are located symmetrically about $c_0 = -\pi$, 0. In this case for $K = 1$ their width is $d = 2\pi/N$. As the distance between 8's increases (Fig. 18a) the centers of the forbidden regions approach each other symmetrically and their width d increases, slowly at first. This pattern of forbidden regions repeats periodically with period 2π. Figure 19 shows an enlarged portion of the principal forbidden region closest to the origin. The boundaries of the forbidden regions are defined in Fig. 18 and 19, the center of one of them in Fig. 19, at $-D$. Dimensions with a single arrow have a sign (for example, d_+ , d_- , D, $\mathbf{D}$), those with two arrows are positive (d, $\mathbf{d}/2$), as before.

From Figs. 18 and 19 and equations 37 through 39 the parameters

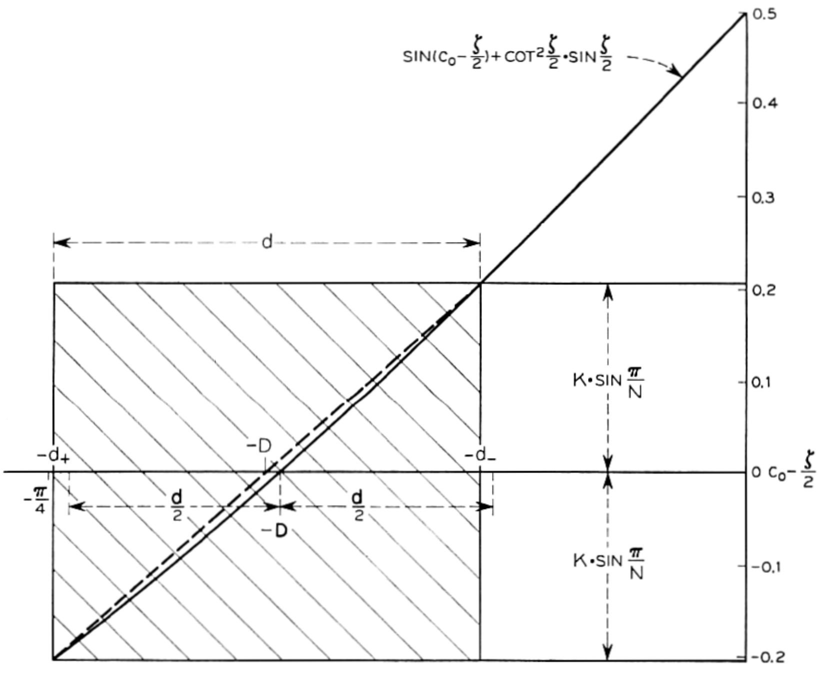

Fig. 19—Enlarged portion of upper curve of Fig. 18a, showing forbidden region closest to origin.

Forbidden Region

Exact	*Approximate*
$D = 30.92°$	$\mathbf{D} = 30°$
$d = 27.55°$	$\mathbf{d} = 27.2°$
$d_- = 17.15°$	$\mathbf{D} - \frac{\mathbf{d}}{2} = 16.4°$
$d_+ = 44.7°$	$\mathbf{D} + \frac{\mathbf{d}}{2} = 43.6°$

defining the forbidden regions are:

$$d_{\pm} = \sin^{-1}\left(\cot^2 \frac{\alpha}{2} \cdot \sin \frac{\zeta}{2} \pm K \sin \frac{\pi}{N}\right). \tag{41}$$

$$D = \frac{d_+ + d_-}{2} \tag{42}$$

$$d = d_+ - d_- . \tag{43}$$

The centers of the principal forbidden regions are located at $-D$, $-(\pi - D)$. In phase space they are located as follows:

$$\begin{aligned} \frac{\zeta}{2} - D - \frac{d}{2} < c_0 < \frac{\zeta}{2} - D + \frac{d}{2}. \\ \frac{\zeta}{2} - \pi + D - \frac{d}{2} < c_0 < \frac{\zeta}{2} - \pi + D + \frac{d}{2}. \end{aligned} \tag{44}$$

The parameter $\cot^2 \alpha/2 \cdot \sin \zeta/2$, which appears throughout the above relations, is a normalized spacing parameter. For such a ζ that the two 8's just touch, $\cot^2 \alpha/2 \cdot \sin \zeta/2 = 1$; therefore, for overlapping 8's this parameter lies between 0 and 1, and for some of the following work where overlapping 8's lie very close together $\cot^2 \alpha/2 \cdot \sin \zeta/2 \ll 1$. Since $\alpha < 30°$, $\zeta/2 < 4.12°$ for overlapping 8's; consequently the approximation $\sin \zeta/2 \rightarrow \zeta/2$ is valid for most purposes.

In the large N case certain approximations are useful. D and d of equations 42 and 43 are approximated by $\mathbf{D}$ and $\mathbf{d}$, given by equations 45 and 46 and illustrated in Fig. 19.

$$\mathbf{D} \equiv \sin^{-1}\left(\cot^2 \frac{\alpha}{2} \cdot \sin \frac{\zeta}{2}\right) \approx D, \qquad N \gg 1. \tag{45}$$

$$\mathbf{d} \equiv \frac{2K \sin \frac{\pi}{N}}{\cos \mathbf{D}} \approx d, \qquad N \gg 1. \tag{46}$$

While these results are not sufficiently precise for all purposes, they serve at least as a rough guide for initial thinking about the problem. For the case illustrated in Fig. 19 ($N = 9$, $K = 0.6$, $\cot^2 \alpha/2 \cdot \sin \zeta/2 = 0.5$) the approximate results of equations 45 and 46 yield a first forbidden region 0.35° too narrow (out of a total width of 27.55°) and 0.92° too far toward the origin. This case has large spacing, and the error will decrease for smaller ζ. In the approximation of equations 45 and 46 the width of the forbidden regions varies linearly with the secant of the displacement of their centers and with the separation reduction factor K, and the location of their centers is independent of K.

A phase-plane picture of the forbidden regions of Figs. 18 and 19 is illustrated in Fig. 20; for later convenience different shading and edges are used to denote the two forbidden regions. For zero spacing, $\zeta = 0$, the forbidden regions have minimum width d and are located symmetrically about 0 and π in the $(c_0 - \zeta/2)$ plane; as ζ increases the forbidden regions approach each other and their width d increases, slowly at first. In Fig. 20a, $K = 1$ and $d > 2\pi/N$ for $\zeta > 0$; in Fig. 20b $K = 0.6$, and for the range of ζ shown $d < 2\pi/N$. It is clear that given an upper bound on ζ, K can be chosen small enough so that $d < 2\pi/N$.

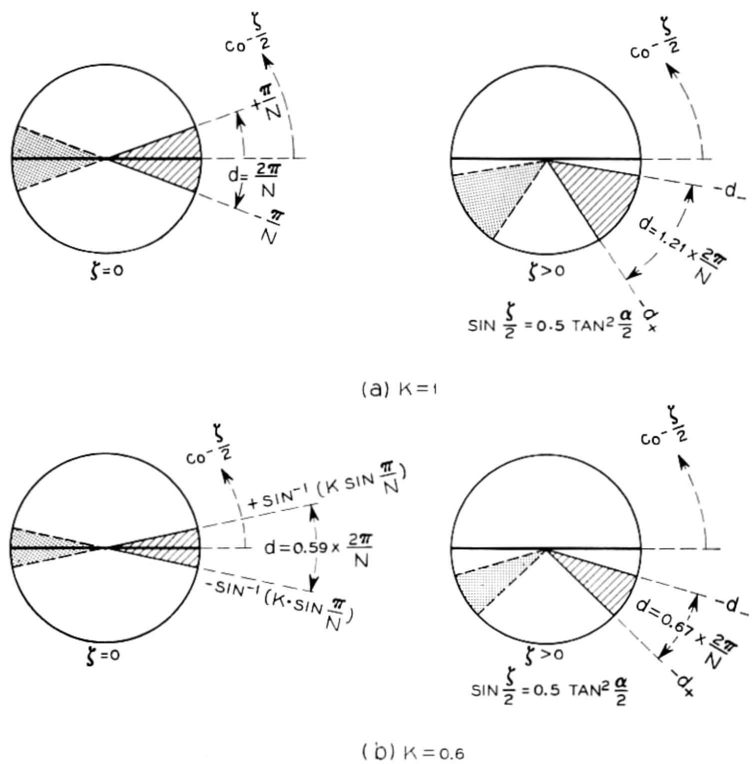

Fig. 20 — Forbidden regions of Figs. 18 and 19 in the $(c_0 - \zeta/2)$ phase plane. $N = 9$. Figures are symmetrical around the vertical axis $(c_0 - \zeta/2 = \pm \pi/2)$.

We now make the additional assumption that each optimally-packed 8 possesses uniform phase spacing over 360°, as in equation 19; this of course implies that N is odd. We inquire whether two or more such 8's can overlap in a useful way, that is, so that improvement factors greater than those of Fig. 17 can be obtained (for the same minimum separation or closest approach). This assumption simplifies the following discussion by rendering all phase-space diagrams N-fold rotationally symmetric, and does yield significant increases in the improvement factor. While superficial study of 180° packing on the individual 8's seems to indicate lower improvement factors in certain simple cases, we have not made a careful study of this alternative case to determine what, if any, advantages it might have. Furthermore, we have not considered other possible (non-180° or non-360° single-8) packing schemes of Section III at all.

Consider the case of two interleaved 8's. The satellite phases on these 8's are (equation 19):

$$\left.\begin{aligned} c_{1(p)} &= c_{1(1)} + 2(p-1)\frac{\pi}{N}, \qquad p = 1, 2, \cdots N; \\ c_{2(q)} &= c_{2(1)} + 2(q-1)\frac{\pi}{N}, \qquad q = 1, 2, \cdots N; \end{aligned}\right\} \quad N \text{ odd.} \tag{47}$$

We define

$$c_0 \equiv c_{2(p)} - c_{1(p)}, \qquad p = 1, 2, \cdots N. \tag{48}$$

All of the c_1's and c_2's vary linearly with time, increasing by 2π in one day. Figure 21a shows the corresponding phase-space plots for each 8, as determined in Section III. In this figure we assume without subsequent restriction that the phase of the $p = 1$ satellite on the left 8 is 0, $c_{1(1)} = 0$. We now inquire what is the optimum value for c_0 (the relative phase between corresponding satellites on the two 8's) to maximize $s_{\min}$, (the closest approach between satellites on different 8's), and thus maximize the packing improvement factor I.

We investigate this question by a mutual phase-space picture derived from Fig. 20. Associated with each of the N satellites on the left 8 (No. 1) there are two forbidden regions in phase space c_2 (or equivalently $c_2 - \zeta/2$ where this is more convenient) determined by a figure such as one of those in Fig. 20. The details depend on the two parameters K (the separation reduction factor of equation 39) and ζ (the equatorial spacing between the two 8's). Figure 20 gives directly the forbidden regions in $c_2 - \zeta/2$ phase space corresponding to

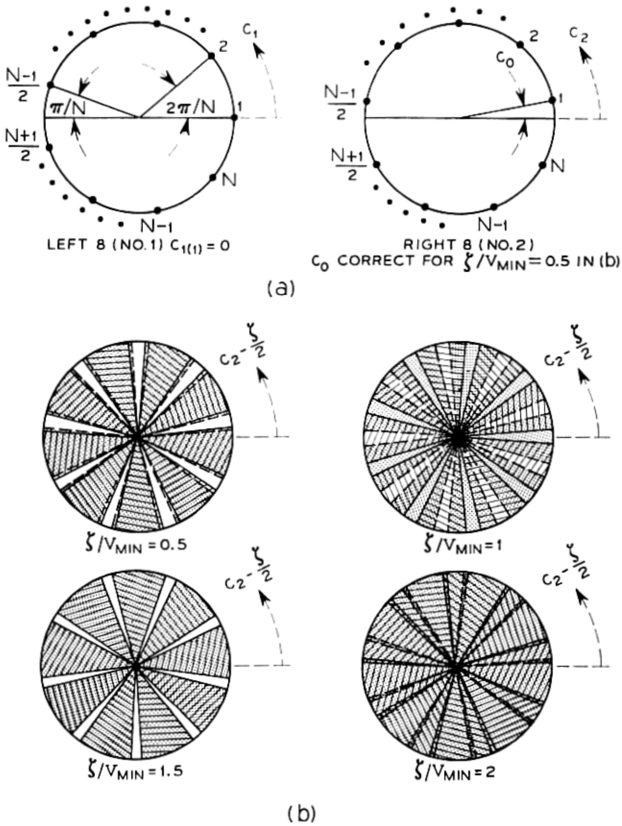

Fig. 21 — Self and mutual phase-space plots for 360° packing on each 8. N is odd, $N = 9$, $\alpha = 30°$, $K = 0.75$. (a) Self phase-space plots for two overlapping 8's. Phase of satellite $1 = 0$ on left 8. (b) Mutual phase-space plot: forbidden regions in $(c_2 - \zeta/2)$ plane determined by satellites in left 8 with phases c_1 of left figure in (a).

the No. 1 satellite on the left 8 in Fig. 21a; the corresponding forbidden regions for the other $(N - 1)$ satellites are determined by rotating such a figure $(N - 1)$ times by an angle $2\pi/N$.

The resulting mutual phase-space picture, shown in Fig. 21b, gives the forbidden and permitted regions for satellites on the right (No. 2)8.* The values of parameters have been chosen in this figure for convenience of illustration, and not necessarily for optimum packing.

* The phase-space plots of Fig. 21 correspond to the particular time at which $c_{1(1)} = 0$; they rotate uniformly counterclockwise, at one revolution per day.

We may imagine that these figures are generated by two spoked wheels rotating in opposite directions on a common shaft. The clockwise rotating wheel has spokes indicated by shading lines, the counter-clockwise wheel by dots, corresponding to the two forbidden regions indicated in the drawings of Fig. 20. Clearly $K < 1$ in order that there be space between spokes for any ζ. As each wheel rotates the spokes widen, and the space between the spokes decreases, finally vanishing ($\zeta/v_{\min} = 2$ in Fig. 21b) as the wheels become solid. Before this happens there are certain angles ($\zeta/v_{\min} = 0.5$, 1.5 in Fig. 21b) at which the spaces between the spokes on the two counter-rotating wheels line up, offering permitted regions for satellites on the second (right) 8.

As indicated in this figure, it proves convenient to normalize the equatorial spacing ζ between 8's to $v_{\min}$, the minimum separation or closest approach on each 8 (equation 38 or 17, or Fig. 13). Figure 21 shows that there are a number of actual or potential "windows" for interleaving two 8's, at spacings of approximately $\zeta/v_{\min} \approx 0.5, 1.5, \cdots$. It is clear that the width of the corresponding permitted regions in c_2-space decreases (and eventually disappears) as the order of the "window" increases, for a fixed K, since the spokes increase in width as ζ increases. Stated differently, the first window (corresponding to the closest spacing for the two 8's) has the highest permitted value of K (such that the width of the permitted regions in c_2-space just approaches zero). Since the highest packing improvement factor corresponds to the largest K, it is clear that best packing (considering only closest approach) is obtained at the first window, that is, with $\zeta/v_{\min} \approx 0.5$ in Fig. 21. It is further clear that a larger value of K than indicated in Fig. 21 can be used.*

Let ζ'' denote the separation between 8's at the first window with the largest possible value of K, such that the permitted regions in c_2-space approach zero width. Then from Figs. 20 and 21

$$d_- = -\frac{\pi}{2N}, \qquad d_+ = +\frac{3\pi}{2N}. \tag{49}$$

From equation 41

$$\sin\frac{\zeta''}{2} = \tan^2\frac{\alpha}{2}\cdot\left[\frac{\sin\frac{3\pi}{2N} - \sin\frac{\pi}{2N}}{2}\right] \tag{50}$$

* Although not shown in Fig. 21, it is clear that for $\zeta = 0$ there are no permitted regions (in c_2 - space) for $K > \frac{1}{2}$. This is the degenerate case in which the two 8's coincide, so that only single-8 packing is effectively considered. The present treatment provides an alternative phase-space derivation to that of Fig. 12 and Section III for the optimum single-8 packing results.

$$K = \frac{\sin \frac{\pi}{2N} + \sin \frac{3\pi}{2N}}{2 \sin \frac{\pi}{N}}. \tag{51}$$

Noting equation 38, an equivalent form of equation 50 that is sometimes useful is

$$\frac{\sin \frac{\zeta''}{2}}{\sin \frac{v_{\min}}{2}} = \sec^2 \frac{\alpha}{2} \cdot \left[\frac{\sin \frac{3\pi}{2N} - \sin \frac{\pi}{2N}}{2 \sin \frac{\pi}{N}} \right]. \tag{52}$$

Finally, the relative phase between corresponding satellites on the two 8's (equation 48) is

$$c_0 = \frac{\pi}{2N} + \frac{\zeta''}{2}. \tag{53}$$

N is odd, of course, throughout equations 49 through 53 (see equation 47). We denote the above geometry by the term "close-spaced interleaved 8's".

Figures 22 and 23 illustrate the spacing between interleaved 8's and the corresponding reduction in minimum separation or closest approach (for satellites on different 8's) for the above conditions. Except for the smallest N, the spacing between 8's ζ'' is close to $v_{\min}/2$, one half the closest approach for satellites on each individual 8, as in the first drawing of Fig. 21b. Similarly, the closest approach $s_{\min}$ for satellites on different 8's is only slightly less than $v_{\min}$ except for the smallest N.* Similar results may be derived for the higher-order windows, but as already mentioned they will have smaller values of K, and hence of the packing improvement factor.

Figure 24 shows the geometric distribution of satellites for two close-spaced interleaved 8's in the region of the equator, at three successive times, for large N. Corresponding satellites on the two interleaved 8's have about the same longitude near the equator, neglecting the factor proportional to $\tan^2 (\alpha/2)$ in satellite phase on the right (dashed) 8. In addition to the two intersections shown near the equator in Fig. 24, the two 8's have two other intersections, near the ends of the 8's, where the satellites must also properly interleave, not

* $s_{\min}/v_{\min}$ is approximately equal to K, as in Fig. 23, to one part in 10^{-4} for the worst case $N = 3$, and to five parts in 10^{-6} for $N \geqq 7$.

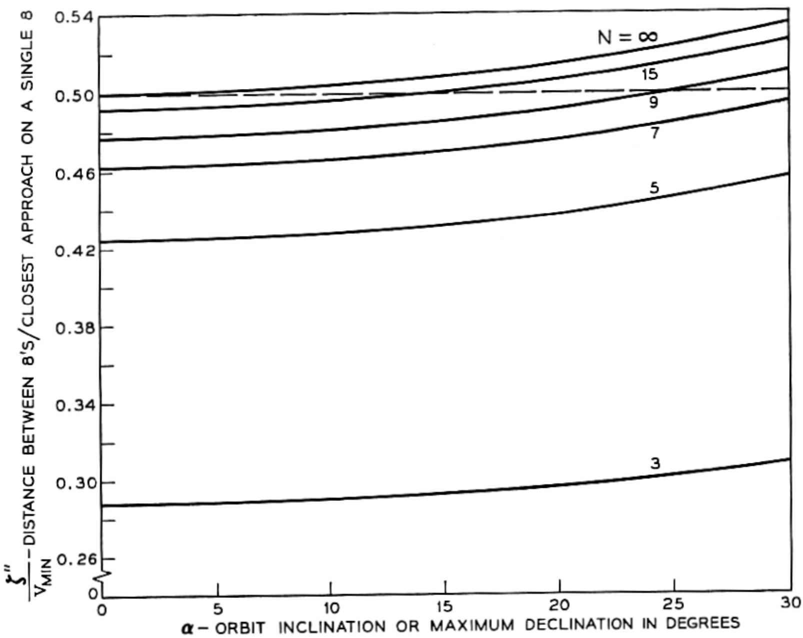

Fig. 22 — Equatorial distance between two close-spaced interleaved 8's. See equations 50 and 52. N = number of satellites on a single 8. N is odd.

shown in Fig. 24. Figure 25 illustrates motion over the complete 8's for a moderate value of N, showing the general nature of closest approaches near all four intersections. Each satellite has 8 closest approaches per day with four different satellites on the other 8 (in addition to four closest approaches per day, with two different satellites on its own 8).

We calculate the improvement factor for such interleaved pairs (close-spaced—that is, at the first "window," $\zeta/v_{\min} \approx 0.5$ for large N) spaced equally along the equator. The $2N$ satellites on each interleaved pair must of course be carefully synchronized; no relative synchronization will be assumed between different pairs.* Two such interleaved pairs are shown in Fig. 26.

The following discussion is quite similar to that of Section IV and

* By synchronizing all of the different pairs they could be placed slightly closer together; indeed, the same is true for the (nonoverlapping) 8's of the packing scheme of Section IV. The phase-space picture given earlier in the present section can easily deal with this problem; however, the possible increase in improvement factor is so slight, particularly for the larger N, that we do not pursue this additional complication here.

Fig. 16; however, the symbols have slightly different definitions here. The closest approach for satellites on different 8's of an interleaved pair, s_{min}, is a little less than v_{min}, the closest approach on each individual 8 (see equation 39 and Fig. 23). Hence the equatorial satellites are assumed to be separated from each other and from the adjacent 8's by s_{min}; the minimum distance between adjacent 8's, u_{min}, must equal or exceed s_{min}; and the equatorial system used for comparison in computing the improvement factor is assumed to have satellites separated by s_{min}. With these changes, and otherwise following the discussion of Section IV, we have:

$$E(\zeta) = \left\{\frac{\zeta - 2\zeta'}{s_{min}}\right\} + 1, \quad \text{number of equatorial satellites between interleaved pairs} \tag{54}$$

where the { } denote "the largest integer contained in" the enclosed

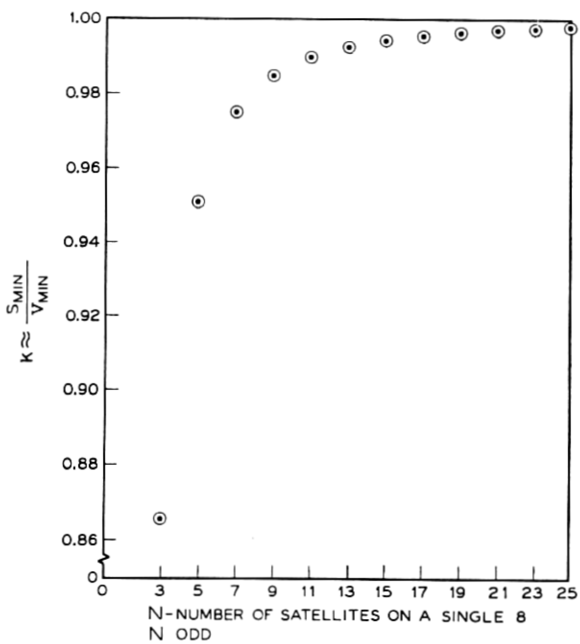

Fig. 23 — Separation reduction factor for two close-spaced interleaved 8's. See equations 51 and 38 through 40.

$\frac{s_{min}}{v_{min}} \approx K$ to graphical accuracy

s_{min} = closest approach for satellites on different 8's

v_{min} = closest approach for satellites on the same 8

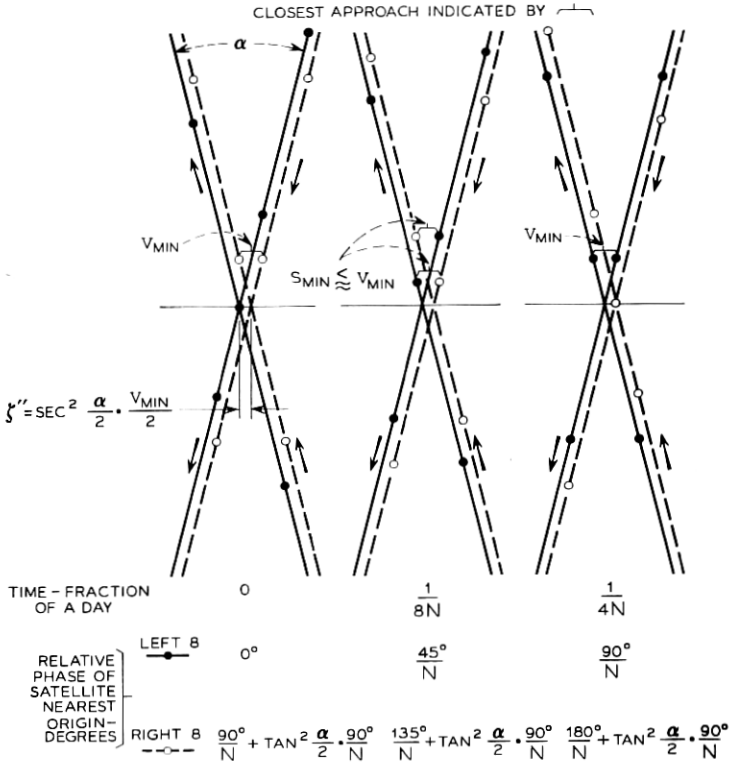

Fig. 24 — Central portion of two close-spaced interleaved 8's. Uniform phase spacing over 360° on each 8. N is odd, N large, $\alpha = 28°$. $\mathrm{Tan}^2\, \alpha/2$ neglected in plotting satellites on right 8.

expression.

$$I(\zeta) = \frac{2N + E}{(\zeta + \zeta'')/s_{\min}} = \frac{(2N + E)s_{\min}}{\zeta + \zeta''}, \qquad \zeta \geqq \zeta_{\min}, \qquad \text{improvement factor.} \tag{55}$$

$$\begin{aligned} I_1 &= I(\zeta_1), \qquad I_2 = I(\zeta_2); \\ \zeta_1 &= \zeta_{\min}, \qquad \zeta_2 = 2\zeta' + s_{\min} \cdot E(\zeta_{\min}). \end{aligned} \tag{56}$$

I_1 corresponds to minimum spacing between adjacent interleaved pairs, I_2 corresponds to just enough extra spacing to accommodate exactly one more equatorial satellite than with minimum spacing.

$$\sin\frac{\zeta'}{2} = \frac{K\sin^2\dfrac{\alpha}{2}\cdot\sin\dfrac{\pi}{N}}{\cos\dfrac{\alpha}{2}}. \tag{57}$$

$$\sin\frac{\zeta_{\min}}{2} = \tan^2\frac{\alpha}{2}\left[1 + K\sin\frac{\pi}{N}\right]. \tag{58}$$

$s_{\min}$ is given by equation 38 and 39 or Fig. 13. In the case of close-spaced interleaved pairs of 8's (that is, using the first "window"), ζ'' is given by equation 50 or 52 or Fig. 22, and K by equation 51 or Fig. 23.

Figure 27 shows the improvement factor in this case in much the same way as Fig. 17 for nonoverlapping 8's. I_1 (corresponding to

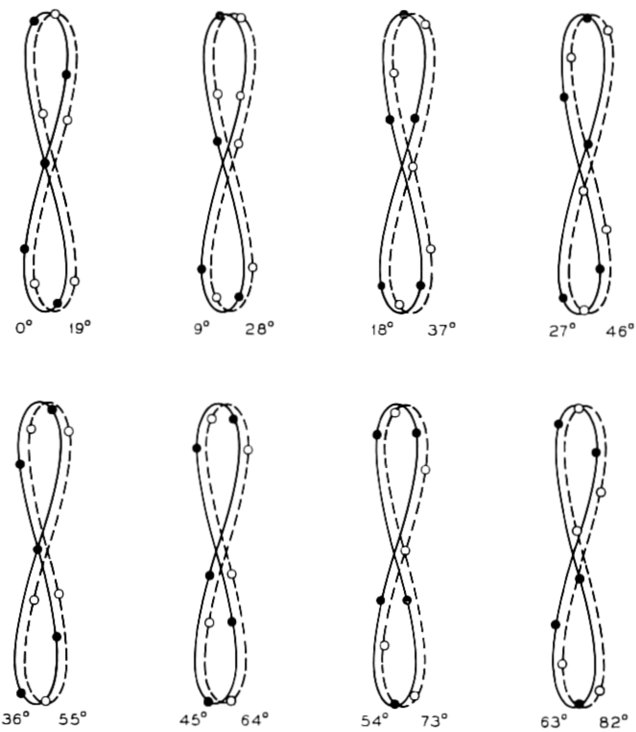

Fig. 25 — Satellite motion for two close-spaced, interleaved 8's. Phases indicated on respective 8's. $N = 5$, $\alpha = 30°$, phase increment $= 9°$, relative phase between two 8's $= 19.03°$.

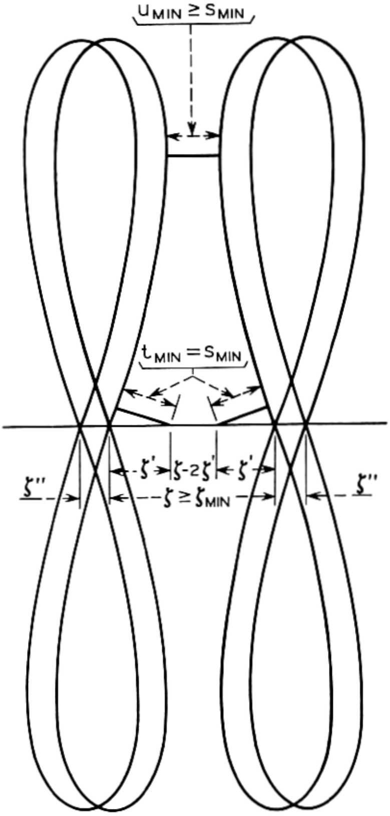

Fig. 26 — Geometry of adjacent interleaved pairs of 8's. $\zeta = \zeta_{min}$ for $u_{min} = s_{min}$. s_{min} = closest approach among $2N$ optimally packed satellites on each interleaved pair of 8's.

minimum separation between adjacent interleaved pairs) is shown by solid lines and I_2 by dashed lines in Fig. 27. However, in contrast to Fig. 17, only the greater of I_1 or I_2, corresponding to the largest improvement factor, is shown. As with the case of Section IV, simpler analytic forms are readily written for $\alpha \to 0$ and $N \to \infty$. We omit the former; the latter yields:

$\underline{N = \infty}$

$$I = I_1 = I_2 = 2\pi \frac{\sin^2 \frac{\alpha}{2}}{\sin^{-1} \tan^2 \frac{\alpha}{2}} + 1. \tag{59}$$

Equation 59 shows that $2\pi + 1$ is an upper bound on the improvement factor for the present packing scheme, as compared with an upper bound of $\pi + 1$ for the scheme of Section IV (compare equation 36). Figure 27 shows that this upper bound, like that of Fig. 17 for the prior scheme, may be approached only for extremely small closest approach (very large N); consequently, practical improvement factors will be somewhat smaller.

The packing scheme of Fig. 27 uses the first "window" for interleaving the overlapping 8's. For N satellites per 8, there are $(N-1)/2$ different windows; expressions analogous to those of equations 49 through 53 (for the first window) are readily written for the higher order windows. There are many different possible packing schemes

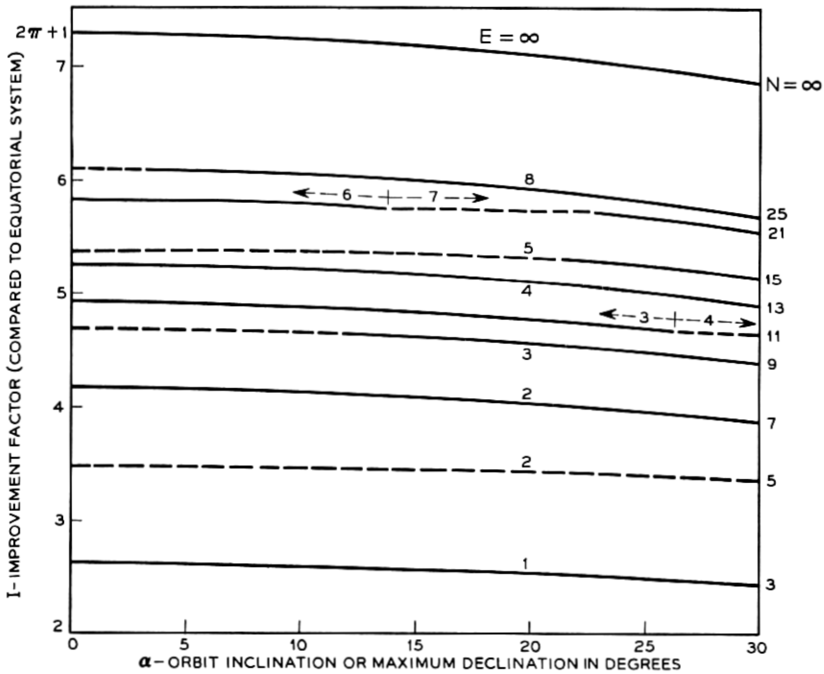

Fig. 27—Improvement factor for optimum satellite packing on separated close-spaced interleaved pairs of 8's. Use this figure in conjunction with Figs. 13, 22, and 23. E = number of satellites on equator between two adjacent interleaved pairs. N = number of satellites on a single 8. N is odd. ———— indicates minimum spacing between adjacent interleaved pairs; closest approach for adjacent pairs = closest approach for a single pair (I_1 of equation 56). – – – indicates increased spacing between adjacent interleaved pairs that just permits 1 additional equatorial satellite (I_2 of equation 56).

using the higher order windows; while it is clear that these have lower improvement factors, some of them may be of interest for other reasons. The improvement factor of this paper is based entirely on closest approach—minimum separation between any pair of satellites. It may pay to degrade this improvement factor in order to increase the average separation between all pairs of satellites in some particular system, for example. Figure 28 shows one possible geometry that will have a somewhat lower improvement factor than the scheme of Fig. 26. The basic relations of this paper permit the study of any of these packing schemes, but we do not pursue this matter further.

In the above examples (Figs. 26 and 27, or 28) only two 8's are effectively interleaved in any given region; consequently, the fairly simple phase-space description of Fig. 21 suffices. We now inquire whether

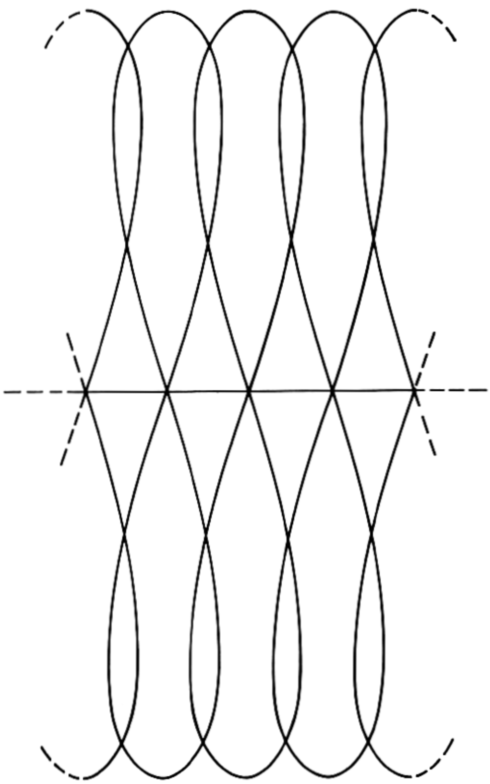

Fig. 28 — Geometry of symmetrically interleaved 8's. Satellites on all 8's must have correct relative phase.

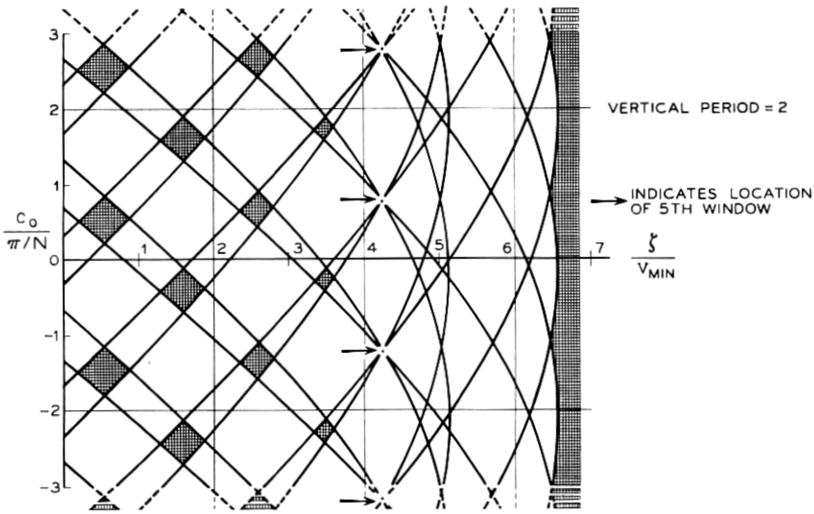

Fig. 29—Windows in the $\zeta - c_0$ plane. $N = 17$, $\alpha = 30°$, $K = 0.674$. K is chosen such that the fifth window is just beginning to open.

Initial Appearance of Window

	Window	K	$\frac{\zeta}{v_{min}}$
	1	0.996	0.529
	2	0.962	1.569
	3	0.895	2.556
	4	0.798	3.456
Present case →	5	0.674	4.239
	6	0.526	4.878
	7	0.361	5.350
	8	0.184	5.640

greater improvement factors than those of Fig. 27 may be attained by using three or more interleaved 8's. We do not know any general technique for investigating this problem, and investigation of a few special cases chosen at random has not produced any significantly greater improvement factor for parameters in the general region of interest ($N \lesssim 25$). Figure 29 is an alternative picture that casts additional light on the general problem of interleaving 8's, even though its use has not yet led to higher improvement factors than those of Fig. 27.

Figure 29 shows a plot of the "windows," or permitted regions of spacing and relative phase between 8's, for a given value of K, the separation reduction factor (and of course given values $N = 17$ and $\alpha = 30°$). The assumptions here are the same as before in this Section, in particular, 360° uniform phase spacing on 8's of identical size (equation 47). Such an 8 may be interleaved with an existing 8 if the equatorial spacing ζ and the relative satellite phase c_0 (equation 48) between the two 8's are such that the corresponding point lies in a shaded region of Fig. 29. For $K = 1$ there are no windows; as K decreases successive windows open up and become larger. As shown by the Fig. 29 table, the first window appears at $K = 0.996$, the second at $K = 0.962, \ldots$, until the fifth appears at $K = 0.674$, corresponding to Fig. 29; as K decreases further, additional windows open up, until all eight are open for $K < 0.184$.

For $\zeta > \zeta_{\min}$ (equation 58) in Fig. 29 for $\zeta/v_{\min} > \zeta_{\min}/v_{\min} = 6.56$, a (nonoverlapping) 8 may be placed with arbitrary relative phase c_0. The border of the shaded region at the right edge of this chart is slightly scalloped; by choosing $c_0/(\pi/N) = 0.85$ the adjacent 8 may be placed a little closer, $\zeta/v_{\min} = 6.45$, but as mentioned in the footnote on page 2412, the potential improvement is so slight (if not nonexistent because it may pay to increase the spacing slightly to accommodate one more equatorial satellite) that we ignore it throughout.

The curves of Fig. 29 are readily obtained from equations 41 through 44 and associated discussion. Four sets of curves must be plotted:

$$c_0 = \begin{bmatrix} \dfrac{\zeta}{2} - d_- \\[2ex] \dfrac{\zeta}{2} + d_- + \dfrac{\pi}{N} \\[2ex] \dfrac{\zeta}{2} - d_+ \\[2ex] \dfrac{\zeta}{2} + d_+ + \dfrac{\pi}{N} \end{bmatrix} + 2(p - 1), \quad p = 1, 2, \cdots N; \quad N \text{ odd}. \tag{60}$$

This figure is periodic in the vertical direction, with period $2\pi/N$ for c_0, as a consequence of the 360° uniform phase spacing assumed on each 8.

A chart such as Fig. 29 may be used to consider the interleaving of a number of 8's in the following manner. Take a number of identical charts, cut out the windows, and cut away the paper to the left of the vertical axis. Lay the first chart down on a light-box. Subsequent charts are now laid down on top, with corresponding axes parallel, in such a way that the origin of each chart always lies on a lighted area. Each chart corresponds to one interleaved 8, so that the total number of charts that can be so laid down equals the number of 8's that can be interleaved for the particular value of K (and of N and α) chosen. The charts must all be translated (with axes parallel), subject to the above constraints, to obtain the maximum total number; the vertical periodicity of these charts greatly reduces the number of possibilities.

After this has been done, if more 8's must be interleaved it will be necessary to repeat the process for a smaller value of K. Since the resulting increase in the number of satellites per unit longitude is accompanied by a decrease in the closest approach $s_{\min}$ (and hence an increase in the denominator of equation 20 defining the improvement factor), it is not obvious, without carrying out this process, whether the improvement factor will be increased or decreased.

It is clear that the process of the preceding two paragraphs does not provide an orderly approach to this problem. A few cases in the region of interest, $N \lesssim 25$, have been tried at random without improving the packing. We recall that since other geometric properties than simply closest approach or minimum satellite separation may be of interest, alternative packing schemes with comparable improvement factors may be of interest; however, we have not pursued these possibilities.

VI. ILLUSTRATIVE SYSTEM SERVING NORTH AMERICA

Figure 30 shows a representative satellite system designed to serve the United States and Canada. While this system has not been optimized, it should serve to illustrate the utility of the above results.

In addition to the general assumptions of Section I, the following general restrictions guided this illustrative design:

(*i*) The most efficient packing scheme that we have devised is used, close-spaced interleaved pairs of 8's (Section V, equation 54 through 59, Figs. 26 and 27).

(*ii*) Closest approach, or minimum separation between any pair of satellites, is about 1°. This would require ground antennas with beamwidths of a fraction of a degree. This might be achieved at frequencies above 12 GHz, possibly in the millimeter band. Such a proposal is somewhat speculative because of the lack of sufficient propagation data.

(*iii*) Minimum elevation above the horizon = 6.4°.

(*iv*) Space in orbit is roughly allocated to what seems the best use.

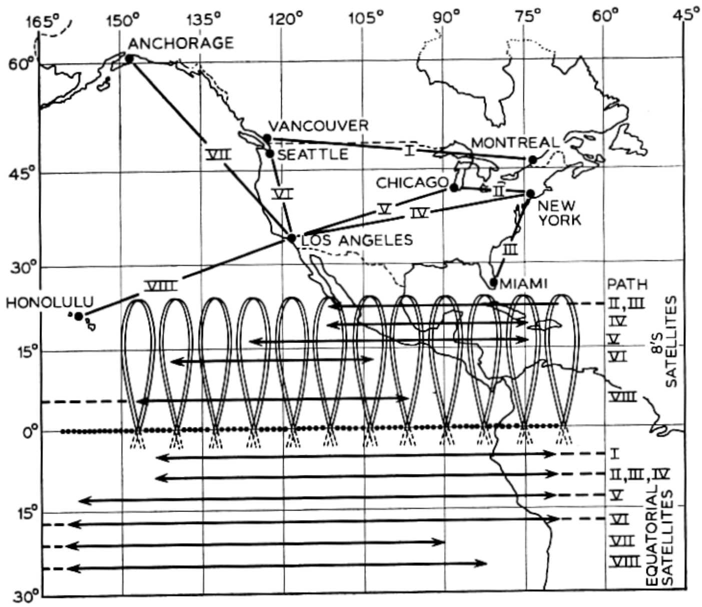

Fig. 30 — Satellite system for North American continent. Total satellites = 477; total in equatorial system occupying same longitude = 95. Packing scheme: close-spaced interleaved pairs of 8's, at minimum spacing ($\zeta = \zeta_{min}$ in Fig. 26). Design parameters: $\alpha = 25°$, orbit inclination. $v_{min} = 0.986°$, $s_{min} = 0.982°$, closest approach. $N = 17$, number of satellites on a single 8 (individual satellites not indicated). $E = 5$, number of equatorial satellites between adjacent pairs of 8's. $I_1 = 5.34$, improvement factor (Fig. 27). Minimum elevation = 6.4°. 8's and equatorial satellites that can serve representative paths without allowing elevation to decrease below 6.4° shown by horizontal arrows, determined from Fig. 32.

Thus, space suitable for trans-Atlantic or trans-Pacific communication has generally not been used. Satellites have been placed farther from the United States coast over the Pacific than over the Atlantic because the Pacific is wider.

(*v*) 8's have been omitted where they would not appear needed (over Hawaii), on the basis of a crude estimate about relative traffic density.

(*vi*) In such a system each satellite might serve every ground station that it can see, within limits imposed by the resolution of the satellite antennas.[1] Referring to Fig. 2, for the minimum elevation chosen for this example (6.4°), an orbit inclination $\alpha = 30°$ allows no tolerance at all in longitude for a ground station at 45° north latitude, somewhat south of the western United States-Canada border.

Consequently, a somewhat smaller inclination ($\alpha = 25°$) has been chosen in Fig. 30.

Figure 31 shows the region of visibility of a satellite from ground stations at several different north latitudes to the same scale as Fig. 30. Equatorial satellites and satellites at 25° south latitude, of interest in Fig. 30, are shown in more detail on Fig. 32.* Using these data, the ranges of 8's and of equatorial satellites that can serve eight representative paths have been shown by the horizontal arrows on Fig. 30.

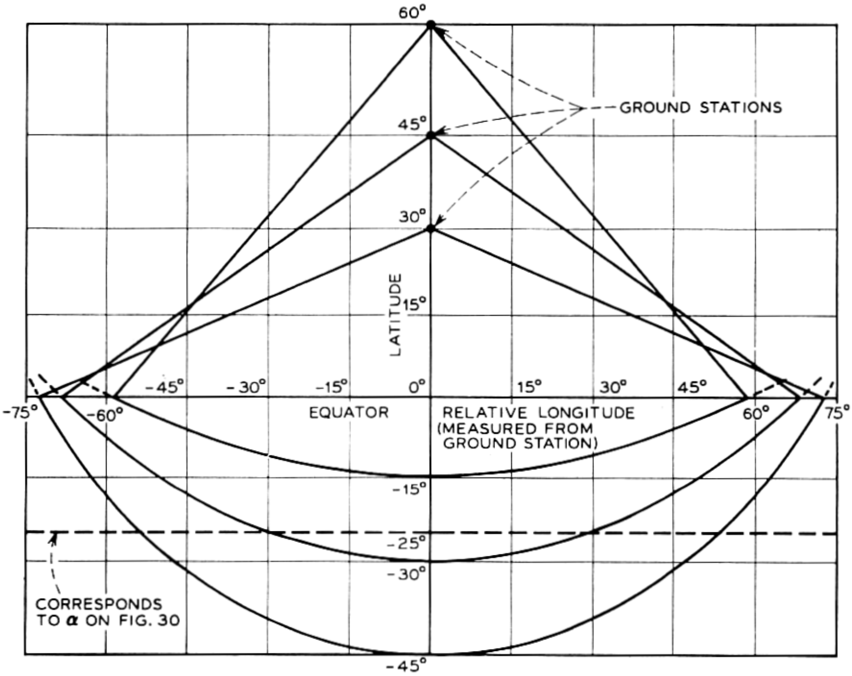

Fig. 31 — Region of visibility of a satellite from ground stations at representative north latitudes, assuming minimum elevation of 6.4° above the horizon. Same scale as Fig. 30, so that these curves give directly permitted 8's and equatorial satellites for representative paths on Fig. 30.

Two general conclusions are readily apparent:

(i) The equatorial satellites are more versatile than the 8's satel-

* The derivation of these results, which is elementary, is given in Appendix B for convenience.

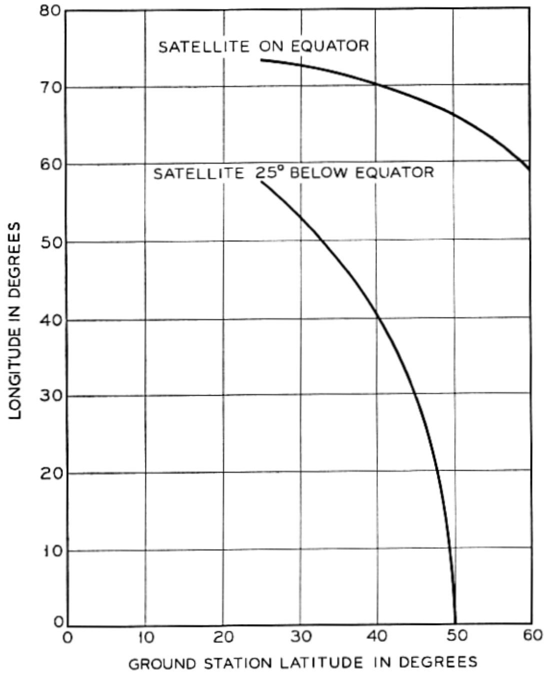

Fig. 32 — Maximum relative longitude from ground station for which satellite is visible 6.4° above the horizon.

lites; only the former can serve paths north of the United States-Canada border.

(*ii*) The most versatile of the 8's satellites lie over the central United States; the further from the center, the smaller the variety of paths served.

Assuming that each satellite carries transponders to serve all ground stations that it can see, the equatorial satellites will be the heaviest, the central 8's satellites next heaviest, and the edge 8's satellites the lightest.

It is obvious that the more easterly satellites of Fig. 30 can also serve Central and South America (with additional transponders for this purpose).

We re-emphasize that this proposed system is only for illustration. Much detailed study would be required to choose the best parameters, even within the assumptions imposed here.

VII. DISCUSSION

The best packing scheme in this paper yields an improvement factor of roughly six over a purely equatorial system in the range of probable interest (see Fig. 27). This result is based on a great many assumptions, already stated. We believe that the relaxation of all of these assumptions should be investigated further. While we have tried to make reasonable choices, we have no assurance either that the improvement factors of Fig. 27 are the best that can be obtained, or that further work will yield better packing schemes (or alternative packing schemes of interest for other reasons).

The treatments of optimum packing a single 8 (Section III) and separated 8's (Section IV) are virtually complete.* However, the treatment of overlapping 8's in Section V, which yields the largest improvement factor, is far from complete. We do not know how to approach this latter problem in a general way. As a start, it seems possible that extending the present treatment of Section V to 8's of moderately different sizes (α's) might allow the interleaving of more than two 8's with significantly greater improvement factors.

All of the discussion has been based on the assumption that each satellite remains in view of every ground station that it serves and no switching is required. This represents one extreme; the other extreme is a low-altitude system, with frequency switching. Intermediate systems are also possible, with switching several times a day. If the assumption is relaxed to allow this, other quite different systems become possible. Two considerations are:

(*i*) Larger 8's (with a larger inclination α) may be used; whether this would lead to any advantage for the United States remains to be studied. However, Europe is enough farther north than the United States that figure 8 systems may not be useful unless occasional switching is allowed.

(*ii*) The antenna scanning and beam shaping problems may be eased. For example with 360° packing on each individual 8, as assumed in the interleaved packing schemes of Section V, each beam would need to scan a much smaller angle.

Once occasional switching is allowed, lower-than-synchronous orbits may be considered. All of the packing schemes discussed above still apply, being based only on circular orbits and not on how fast the

* Not all items of interest have been investigated, but we believe the basic relations given here are sufficient for most purposes.

earth happens to be rotating. However, now the satellite would have to extend all the way around the earth, rather than say one quarter of the way around as in Fig. 30 for synchronous orbits. Further, the mutual visibility problem becomes worse as the altitude decreases; additional study would be required to determine the resulting improvement factors.

In Sections IV and V different 8's and different interleaved pairs of 8's, respectively, were allowed to have arbitrary relative phase. We now inquire what use can be made of this additional parameter. As already mentioned, slightly closer packing and hence slightly greater improvement factors can be obtained in some cases by the correct choice of relative phase, although this increase is small and will yield only a few additional satellites in the illustrative system of Fig. 30.

A more interesting possibility is to use this parameter to reduce the number of different orbits required, so that one vehicle can launch many different satellites lying on the same orbit but on different 8's. From the basic definitions of Fig. 4, it is obvious that two satellites lying on the same orbit but on different 8's of identical size (α), spaced along the equator by ζ, have a relative phase of ζ. The $2 \times 12 \times 17 = 408$ 8's satellites of Fig. 30 generally require 408 orbits. By proper choice of relative phase ($\zeta + \zeta'' =$ phase difference between adjacent pairs—see Fig. 26), only 34 different orbits are required; thus only 34 launch vehicles, each carrying 12 satellites, need be used.

A study of the fuel requirements to maintain desired tolerances in satellite positions for the different systems is needed. It is not obvious whether this requirement is greatly different for the different systems.

VIII. ACKNOWLEDGMENT

The authors thank L. C. Tillotson for suggesting this problem and for many helpful discussions, and Mrs. Evelyn Kerschbaumer for programming computer movies illustrating satellite motion.

APPENDIX A

Derivation of Fundamental Results of Section II

Consider on Fig. 4 the isosceles (spherical) triangle composed of the equator, the orbit, and the great circle connecting the satellite to the earth reference point (at the intersection of the reference longitude and the equator). This triangle has two equal sides of (great circle) length

c (measured by the angle subtended at the center of the sphere) with included angle α, and a third side of length a; let the remaining two equal angles be denoted by γ (not indicated on Fig. 4). Noting that $\gamma + \epsilon = \pi/2$, the law of sines yields

$$\frac{\sin \alpha}{\sin a} = \frac{\cos \epsilon}{\sin c}. \tag{61}$$

Now bisect the above triangle into two equal right triangles by bisecting the angle α (with a great circle). From the law of sines

$$\frac{\sin \frac{\alpha}{2}}{\sin \frac{a}{2}} = \frac{1}{\sin c}, \tag{62}$$

which yields equation 1. We now use equation 1 to eliminate the parameter a from equations 61 by means of the double-angle formula, yielding

$$\cos \epsilon = \left[\frac{1 - \sin^2 \frac{\alpha}{2}}{1 - \sin^2 \frac{\alpha}{2} \cdot \sin^2 c} \right]^{\frac{1}{2}}. \tag{63}$$

Equation 2 now follows directly.

Equation 3 follows from the law of sines applied to the right triangle of Fig. 4 whose sides are the orbit, the equator, and the dotted longitude passing through the satellite. The law of cosines applied to this triangle yields

$$\cos c = \cos l \cdot \cos e. \tag{64}$$

This becomes

$$\sin e = \left(\frac{\sin^2 c - \sin^2 l}{1 - \sin^2 l} \right)^{\frac{1}{2}}; \tag{65}$$

substituting equation 3 into equation 65 yields equation 5.

Consider next the right triangle formed by the equator, the dotted longitude, and the great circle joining the satellite to the earth reference point (defined in the first sentence of this appendix) in either Fig. 4 or 6. The law of cosines yields

$$\cos a = \cos l \cdot \cos \psi. \tag{66}$$

Thus

$$\sin \psi = \left(\frac{\sin^2 a - \sin^2 l}{1 - \sin^2 l} \right)^{\frac{1}{2}}. \tag{67}$$

Using the double-angle formula, substituting equations 1 and 3 into equation 67 yields equation 4.

Consider now the right triangle of Fig. 6 formed by the reference longitude, the great circle connecting the satellite to the earth reference point (see above), and the great circle of length x passing through the satellite and normal to the reference longitude. From the law of sines

$$\sin x = \sin a \cdot \sin \epsilon. \tag{68}$$

Using equations 1 and 2 to eliminate α and ϵ, together with the double angle formula, equation 7 is readily obtained.

We next derive the general result of equation 11, obtaining all the remaining results of Section II by specializing this relation. Applying the law of cosines to the spherical triangle of Fig. 9 whose vertices are the north pole and the satellites on each of the two 8's,

$$\cos s = \sin l_1 \cdot \sin l_2 + \cos l_1 \cdot \cos l_2 \cdot \cos (\zeta + \psi_1 - \psi_2). \tag{69}$$

Make the following substitutions in equation 69:

(*i*) equation 3.

(*ii*) Expand $\cos (\zeta + \psi_1 - \psi_2)$.

(*iii*) From equations 66 and 1, and the double-angle formula,

$$\cos l \cdot \cos \psi = 1 - 2 \cdot \sin^2 \frac{\alpha}{2} \cdot \sin^2 c$$

$$= \cos^2 \frac{\alpha}{2} + \sin^2 \frac{\alpha}{2} \cdot \cos 2c$$

(*iv*) From equations 3 and 4

$$\cos l \cdot \sin \psi = \sin^2 \frac{\alpha}{2} \cdot \sin 2c.$$

After lengthy but straightforward transformations equation 11 is obtained. We readily obtain equation 8 (see Fig. 6) by the second transformation in the table following equation 11. For equation 10, the fourth transformation of this table yields

$$\cos u = \cos \zeta \cdot \cos^4 \frac{\alpha}{2} + \frac{\sin^2 \alpha}{2} [\cos (2c_2 - \zeta) - \cos 2c_2] + \frac{\sin^2 \alpha}{2} + \sin^4 \frac{\alpha}{2} \cdot \cos (4c_2 - \zeta). \tag{70}$$

Make the following substitutions in equation 70:

(*i*) $\cos (2c_2 - \zeta) - \cos 2c_2 = 2 \sin \left(2c_2 - \frac{\zeta}{2}\right) \cdot \sin \frac{\zeta}{2}.$

(*ii*) $\cos \sigma = 1 - 2 \sin^2 \frac{\sigma}{2}; \qquad \sigma = u, \zeta, 4c_2 - \zeta.$

(*iii*) $\frac{\sin^2 \alpha}{2} = 2 \sin^2 \frac{\alpha}{2} \cdot \cos^2 \frac{\alpha}{2}.$

We have after combining terms

$$\sin^2 \frac{u}{2} = \left[\cos^2 \frac{\alpha}{2} \cdot \sin \frac{\zeta}{2} - \sin^2 \frac{\alpha}{2} \cdot \sin \left(2c_2 - \frac{\zeta}{2}\right)\right]^2, \tag{71}$$

simply the square of equation 10.

To derive equation 13, substitute equation 12 into equation 11 and use the double-angle formula on the α-dependent factors of the third and fourth terms to yield, after some minor rearrangement,

$$\cos s = \cos \zeta \cdot \cos^4 \frac{\alpha}{2} + \sin^4 \frac{\alpha}{2} \cdot \cos (2c_0 - \zeta) + \frac{\sin^2 \alpha}{2} \cdot \cos c_0 + \frac{\sin^2 \alpha}{4} [\cos (2c_1 + c_0 - c_0 + \zeta) + \cos (2c_1 + c_0 + c_0 - \zeta) - 2 \cos (2c_1 + c_0)]. \tag{72}$$

The three terms inside [ ] may be regarded as an AM wave and so are readily combined, to yield

$$\cos s = \cos^4 \frac{\alpha}{2} \cdot \cos \zeta + \sin^4 \frac{\alpha}{2} \cdot \cos (2c_0 - \zeta) + \frac{\sin^2 \alpha}{2} \cdot \cos c_0 - \sin^2 \alpha \cdot \sin^2 \left(\frac{c_0 - \zeta}{2}\right) \cdot \cos (2c_1 + c_0). \tag{73}$$

Make the following substitutions in equation 73:

(*i*) $\cos \sigma = 1 - 2 \sin^2 \frac{\sigma}{2}; \qquad \sigma = s, \zeta, 2c_0 - \zeta, c_0.$

$$(ii) \qquad \cos(2c_1 + c_0) = 2\cos^2\left(c_1 + \frac{c_0}{2}\right) - 1.$$

$$(iii) \qquad \frac{\sin^2 \alpha}{2} = 2\sin^2\frac{\alpha}{2}\cdot\cos^2\frac{\alpha}{2}.$$

Equation 13 is obtained directly. Equation 9 follows immediately, as pointed out in the text.

There are of course a great many alternate ways of deriving these various results.

APPENDIX B

Visibility of a Satellite from a Ground Station

Figure 33 shows the earth, of unit radius, concentric with a sphere of radius R, equal to the radius of a circular satellite orbit. For syn-

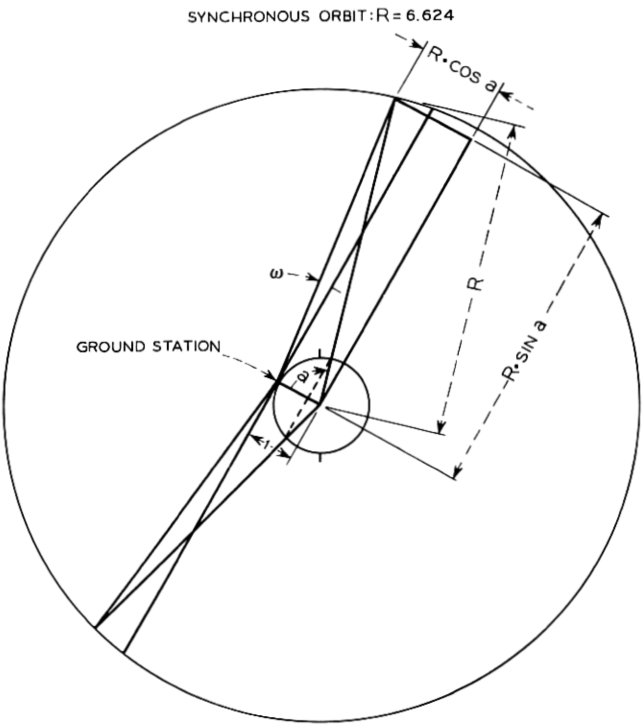

Fig. 33 — Region of visibility of a satellite. Synchronous orbit: $R = 6.624$.

chronous orbits $R = 6.624$. The elevation of a satellite viewed from a ground station must exceed the angle ω; the satellite is restricted to a region of angle from the ground station (measured at the center of the spheres) less than a. Projecting the satellite on a sphere (the earth in Fig. 33), the satellite is restricted to a region within a circle centered on the ground station (shown dashed in Fig. 33) of (great circle) radius a, with the usual convention of spherical trigonometry that great circle distances are measured by the angle they subtend at the center of the sphere. From Fig. 33,

$$\tan \omega = \frac{R \cdot \cos a - 1}{R \cdot \sin a} = \cot a - \frac{\csc a}{R}. \tag{74}$$

Solving for a,

$$\sin a = \cos \omega \left[1 - \left(\frac{\cos \omega}{R}\right)^2\right]^{\frac{1}{2}} - \frac{\sin 2\omega}{2R}. \tag{75}$$

At synchronous radius,

$$\sin a = \cos \omega (1 - .0228 \cos^2 \omega)^{\frac{1}{2}} - 0.0755 \sin 2\omega,$$

$$R = 6.624. \tag{76}$$

The relation between latitude l and relative longitude ψ on the dotted circle is found from Fig. 34. The ground station is located at north latitude l_0. From the law of sines,

$$\cos l \cdot \sin \psi = \sin a \cdot \sin \epsilon. \tag{77}$$

From the law of cosines

$$\sin l = \cos a \cdot \sin l_0 + \sin a \cdot \cos l_0 \cdot \cos \epsilon. \tag{78}$$

Substituting equation 76 into equations 77 and 78, the results of Figs. 31 and 32 are readily computed parametrically in terms of the azimuth ϵ.

APPENDIX C

Error in Satellite Separation

The error in separation between satellites resulting from displacement from the center of the earth is readily calculated. Fig. 35 shows the earth and a pair of satellites in circular orbits of radius R, separated at this instant by angle s subtended at the center of the earth. The side view shows a ground station; the plane of the paper includes

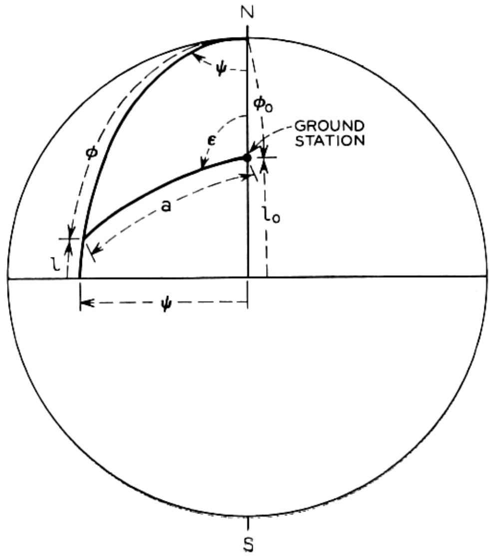

Fig. 34 — Latitude and longitude of region of visibility.

the center of the earth, the ground station, and the upper satellite. The poles of the earth are not necessarily vertical in this figure. The lower satellite does not in general lie in the plane of the paper; the end view shows a line joining the two satellites, making an angle τ with the plane of the upper satellite, ground station, and center of the earth.

In the case of interest here the satellites lie close together. Con-

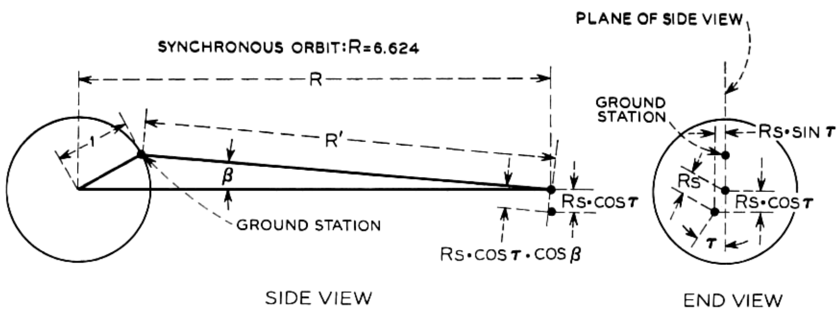

Fig. 35 — Satellite separation as a function of ground station location. s = angular separation between satellites at center of earth. Distance between satellites (Rs) and its projections are true (not angular) lengths.

sequently we assume throughout this appendix that

$$s \ll 1. \tag{79}$$

The ground station is restricted to the region of the earth where the satellite remains visible, the limiting case corresponding to zero elevation.* Consequently the angle β of Fig. 35 is bounded by

$$\beta < \beta_{\max}, \qquad \sin \beta_{\max} = 1/R. \tag{80}$$

The distance R' from the ground station to the satellite has maximum and minimum values corresponding to maximum and minimum values of β. Thus

$$1 - \frac{1}{R} < \frac{R'}{R} < \cos \beta_{\max} = \left(1 - \frac{1}{R^2}\right)^{\frac{1}{2}}. \tag{81}$$

We seek the angular separation between the two satellites as seen from the ground station; let this quantity be denoted by s'. We project the line segment joining the two satellites onto the plane perpendicular to the line R' joining the satellites and the ground station as shown. Then

$$s'/s = (R/R')[1 - (\sin \beta \cdot \cos \tau)^2]^{\frac{1}{2}}. \tag{82}$$

We have

$$1 < s'/s < \frac{R}{R - 1}. \tag{83}$$

For synchronous orbit

$$1 < s'/s < 1.178. \tag{84}$$

Thus as stated in Section I, for synchronous orbit the approximation of this paper which determines separation between satellites as seen from the center of the earth (rather than from ground stations) ranges from correct to 18 per cent too conservative for the critical cases of closest approach.

REFERENCE

1. Tillotson, L. C., "A Model of a Domestic Satellite Communication System," B.S.T.J., this issue, pp. 2111–2137.

* Practically the minimum elevation must be greater than zero, as in Appendix B. A minimum elevation of 6.4° was assumed in Section VI.